Guided Wave Optics Laboratory

Report No. 71

Scattering-Induced Crosstalk
in Active Directional Couplers

S. Lin, W. Feng, J. C. Powelson, R. J. Feuerstein,
L. Bintz, D. Tomic, and A. R. Mickelson

February 27, 1996

Department of Electrical and Computer Engineering

University of Colorado at Boulder
Boulder, Colorado

Report No. 71

Scattering-Induced Crosstalk in Active Directional Couplers

S. Lin, W. Feng, J. C. Powelson, R. J. Feuerstein,
L. Bintz, D. Tomic, and A. R. Mickelson

February 27, 1996

Guided Wave Optics Laboratory
Department of Electrical and Computer Engineering
University of Colorado at Boulder
Boulder, Colorado 80309-0425

This work was supported by the Advanced Research Projects Agency (ARPA) under grant number MDA972-93-1-0007 through a subcontract of IBM, the Army Research Office (ARO) under grant number DAAL-03-92-G0289, the Office of Naval Research (ONR) under grant number N00014-95-I-0494, and the Air Force Rome Laboratories under grant number F30602-95-C-0227. J. C. Powelson would like to acknowledge a doctoral fellowship provided by AT&T.

unclassified
SECURITY CLASSIFICATION OF THIS PAGE

DISTRIBUTION STATEMENT A
Approved for public release
Distribution unlimited

REPORT DOCUMENTATION PAGE

Form Approved
OMB No. 0704-0188

1a. REPORT SECURITY CLASSIFICATION: unclassified	1b. RESTRICTIVE MARKINGS: none
2a. SECURITY CLASSIFICATION AUTHORITY: DISCASS	3. DISTRIBUTION / AVAILABILITY OF REPORT: ~~unrestricted~~
2b. DECLASSIFICATION / DOWNGRADING SCHEDULE: N/A	
4. PERFORMING ORGANIZATION REPORT NUMBER(S): ECE/GWOL/ 71	5. MONITORING ORGANIZATION REPORT NUMBER(S): DOD-ONRN00014-92-J-1190
6a. NAME OF PERFORMING ORGANIZATION: University of Colorado; 6b. OFFICE SYMBOL (If applicable):	7a. NAME OF MONITORING ORGANIZATION: Office of Naval Research, Attn: Dr. Arthur Jordan, Code 1114 SE
6c. ADDRESS (City, State, and ZIP Code): Electrical & Computer Engineering Dept., Boulder, CO 80309-0425	7b. ADDRESS (City, State, and ZIP Code): 800 N. Quincy Avenue, Arlington, VA 22217-5000
8a. NAME OF FUNDING / SPONSORING ORGANIZATION: Office of Naval Research; 8b. OFFICE SYMBOL (If applicable):	9. PROCUREMENT INSTRUMENT IDENTIFICATION NUMBER:
8c. ADDRESS (City, State, and ZIP Code): 800 N. Quincy Avenue, Arlington, VA 22217-5000	10. SOURCE OF FUNDING NUMBERS: PROGRAM ELEMENT NO. / PROJECT NO. / TASK NO. / WORK UNIT ACCESSION NO.

11. TITLE (Include Security Classification)

(u) Scattering-Induced Crosstalk in Active Directional Couplers

12. PERSONAL AUTHOR(S)
S. Lin, W. Feng, J. C. Powelson, R. J. Feuerstein, L. Bintz, D. Tomic, A. Mickelson

13a. TYPE OF REPORT	13b. TIME COVERED	14. DATE OF REPORT (Year, Month, Day)	15. PAGE COUNT
manuscript	FROM _____ TO _____	2/27/96	51

16. SUPPLEMENTARY NOTATION

17. COSATI CODES			18. SUBJECT TERMS (Continue on reverse if necessary and identify by block number)
FIELD	GROUP	SUB-GROUP	

19. ABSTRACT (Continue on reverse if necessary and identify by block number)

Scattering from defects in an integrated optical device causes phase randomization and depolarization. Scattered light can be recaptured by the waveguides of the device and perturbs modal fields. This leads to crosstalk in directional coupler switches. A defect-scattering-induced crosstalk model is developed, and crosstalk in one-, two-, and three-electrode directional couplers is investigated with the model. The number of independent electrode voltages needed to tune out crosstalk is studied. Simulations show that scattering-induced crosstalk can be tuned out completely in active directional couplers with two independent electrode voltages. When modal differential loss and unequal taper coupling are taken into account, two independent electrode voltages are insufficient to tune out the crosstalk, whereas three independent electrode voltages are sufficient. This agrees with the conclusion from three-electrode directional coupler experiments.

20. DISTRIBUTION / AVAILABILITY OF ABSTRACT: ■ UNCLASSIFIED/UNLIMITED ☐ SAME AS RPT. ☐ DTIC USERS	21. ABSTRACT SECURITY CLASSIFICATION: unclassified
22a. NAME OF RESPONSIBLE INDIVIDUAL: Alan R. Mickelson	22b. TELEPHONE (Include Area Code): 303/492-7539; 22c. OFFICE SYMBOL:

DD Form 1473, JUN 86 — Previous editions are obsolete. — SECURITY CLASSIFICATION OF THIS PAGE

Scattering Induced Crosstalk in Active Directional Couplers *

Sihan Lin, Wei Feng, Judith C. Powelson, Robert J. Feuerstein
Lou Bintz, Darja Tomic, and Alan R. Mickelson

Department of Electrical and Computer Engineering
University of Colorado, Boulder, CO 80309

February 27, 1996

Abstract

Scattering from defects in an integrated optical device causes phase randomization and depolarization. Scattered light can be recaptured by the waveguides of the device and perturbs modal fields. This leads to crosstalk in directional coupler switches. A defect-scattering-induced crosstalk model is developed and crosstalk in one-, two-, and three-electrode directional couplers is investigated with the model. The number of independent electrode voltages needed to tune out crosstalk is studied. Simulations show that scattering-induced crosstalk can be tuned out completely in active directional couplers with two independent electrode voltages. When modal differential loss and unequal taper coupling are taken into account, two independent electrode voltages are insufficient to tune out the crosstalk, whereas three independent electrode voltages are sufficient. This agrees with the conclusion from three-electrode directional coupler experiments [1].

*This work is supported by Advanced Research Projects Agency (ARPA) under grant number MDA972-93-1-0007 through a subcontract of IBM, Army Research Office (ARO) under grant number DAAL-03-92-G0289, Office of Naval Research (ONR) under grant number N00014-95-I-0494, and Airforce Rome Laboratories under grant number F30602-95-C-0227. J. C. Powelson would like to acknowledge a doctoral fellowship provided by AT&T.

1 Introduction

Crosstalk of directional coupler switches limits the performance of optical switching networks. In digital communication systems, better than -15 dB crosstalk is required to achieve an acceptable bit error rate (BER). In analog optical communication systems, the crosstalk of each switch needs to be better than -30 dB. In cable TV applications, better than -60 dB interchannel electrical crosstalk is required. If one uses optical switching networks, in which photodetectors convert optical power to voltage, an equivalent -30 dB optical crosstalk is required to obtain a -60 dB electrical crosstalk for directional coupler switches.

Elimination of crosstalk in optical switches has remained an interesting research topic for years [2] [3]. Numerous efforts have been made to understand the cause and reduction of crosstalk in directional coupler switches [4] [5] [6] [7].

Crosstalk can be attributed to several sources. A nonoptimum coupling length of a device induces crosstalk [8]. For passive directional couplers, this can be corrected through a fine-tuning process such as annealing of Ti:$LiNbO_3$ devices or UV bleaching of nonlinear optical polymer devices. In active directional couplers, the electro-optic (EO) effect allows voltage tuning of the coupling length of the devices. Reversed-$\Delta\beta$ directional couplers were proposed [9] and implemented [6] with the expectation of low crosstalk and high production yield. For active devices, a nonoptimum coupling length can be adjusted through voltage tuning of a reversed-$\Delta\beta$ coupler with only one voltage source. However, DC drift [10] [11] in active couplers adds complexity and introduces time dependent coupling length variations and asymmetric mode conversions in two electrode sections. Two adjustable DC bias voltages have been used on reversed-$\Delta\beta$ couplers to tune out the time dependent variations in order to achieve better crosstalk levels [12].

It is desirable for two waveguides in a directional coupler to be identical. If the index profiles or the channel widths of the two guides are not exactly the same, an asymmetry is introduced. Asymmetry of the waveguides produces mode conversion between the symmetric

and antisymmetric modes in the taper region, resulting in crosstalk [13]. For a directional coupler with a few millimeters coupling length, less than 1% asymmetry produces greater than -20 dB crosstalk [14]. However, with state-of-the-art IC technology this effect is minimal.

Coupling in the taper region lowers the performance of reversed-$\Delta\beta$ directional coupler switches [15] [16]. A tapered electrode structure has been proposed as a solution [3]. Unequal excitation of symmetric and antisymmetric modes from an input guide can also lead to crosstalk [17]. Tapered coupling structures may be able to eliminate it [2].

Absorption loss induced crosstalk was first discussed in [18]. Optical scattering also causes loss. Since the modal profiles of the two guided modes are different, they may experience different propagation losses, and this differential loss can be another source of crosstalk [19].

Waveguide inhomogeneities due to defects along the waveguides result in crosstalk. Channel waveguides fabricated with wet etching or dry etching have rough sidewalls, which cause index variations along waveguides. Any defects in the waveguide material also result in index perturbations. They can generate an index variation directly such as at crosslink centers in polymer waveguides made of epoxy type of materials, which are denser and have a higher index of refraction than other regions. Defects can also vary the index profile indirectly. In Ti-indiffused channel waveguides, index variation is generated by a defect induced nonuniform diffusion constant of Ti. The Ti concentration inhomogeneity in $LiNbO_3$ waveguides was measured with an electron probe [20]. Studies of random-index-perturbation induced crosstalk due to such defects along the waveguides in Ti-indiffused $LiNbO_3$ directional couplers [1] [4] have shown that an index perturbation of one part in 10^4 results in about -30 dB crosstalk [4]. Defects can also perturb the EO coefficient. In reversed-$\Delta\beta$ directional coupler devices, domain inversion varies the local EO coefficient, causing a different phase change in each section of the $\Delta\beta$ reversal switch, degrading performance of the device [21].

A directional coupler is an interferometric device. The two coupled modes in the device need to have equal amplitudes and to be in or out of phase when they decouple at the output in order to have zero crosstalk for the bar and the cross states respectively. The perturbation due to waveguide inhomogeneities changes either the relative phase or the relative amplitude, or perhaps both. To reduce crosstalk it is necessary to tune both the relative phase and the

relative amplitude of the two coupled modes. As mentioned above, two DC bias voltages on the reversed $\Delta\beta$-directional coupler have been used to improve the crosstalk. A phase compensation technique through tailoring the two electrodes [7] [22], and current injection into semiconductor material [7] have also been used in such devices, and -38 dB crosstalk has been achieved in both bar and cross states [7]. Crosstalk has been further improved by employing three-electrode structures [1], with a crosstalk of -47.8 dB observed in the bar state.

In the random-index-perturbation induced crosstalk model [1] [4] the coupled mode equations were used to calculate the perturbation to the phases and amplitudes of the modes, so that only the coupling between the two ideal modes was evaluated, and coupling into the radiation modes was neglected. Identically fabricated devices don't have the same crosstalk value, and the crosstalk values have a distribution within a 20 dB range [23]. This large distribution is attributed to a random process in the devices. Defects in the waveguides differ from one device to another. The defects in the devices can be the cause of the crosstalk distribution. We will show in this article that random defects in devices can explain the observed crosstalk distributions.

Instead of considering the random perturbation of the index in the guides, we use an alternative model for the defects. It is well known that defects inside waveguides cause scattering of the modal light [18]. Scattered light can be recaptured by the waveguides. Scattering causes random phase delay and depolarization. Captured scattered light from different scatterers adds up coherently with the unscattered light in the guides, perturbing both the relative phase and the relative amplitudes of the two coupled modes, resulting in crosstalk. Since the defects are different from device to device, the perturbation from the captured scattered light results in a distribution of crosstalk values.

In this article we report a study of crosstalk due to defect scattering in one-, two- and three-electrode directional coupler switches. We discuss how voltage tuning can be used to eliminate crosstalk due to defect scattering, unequal coupling into symmetric and antisymmetric modes, taper coupling, and the modal differential loss in waveguides. The degrees of freedom necessary to tune out the crosstalk are also discussed. Due to limited space, only cross-state crosstalk is presented, but similar results apply to bar-state crosstalk.

2 Coupled Mode Theory

2.1 Coupled Mode Equations

Fig. 1 shows a conventional directional coupler. Coupled mode theory can be employed to calculate the evolution of light in directional couplers [22] [24]. The scalar coupled mode equations are commonly used in guided wave optics since eigenmodes of waveguides are either TE or TM and the eigen fields can be treated as scalar fields. In the interaction region, two waveguide modes are coupled. With no voltage applied the two modes are symmetric and antisymmetric modes. With voltage applied to the electrodes, the electro-optic effect causes the index of refraction to increase in one guide and decrease in the other, so the two eigenmodes are no longer symmetric or antisymmetric. The difference of the propagation constants of the two eigenmodes changes, which allows the directional coupler to switch.

Assume that $\Psi_{0s}(x,y)$ and $\Psi_{0a}(x,y)$ are the symmetric and antisymmetric normalized modal fields in the interaction region with no voltage applied. The modal field is normalized as

$$\int_{-\infty}^{\infty} \mid \Psi_i(x,y) \mid^2 \, dxdy = 2\eta_i, \tag{1}$$

where $\eta_i = \eta_0 k_0/\beta_i$ is the effective impedance of the ith mode, $\eta_0 = \sqrt{\mu_0/\varepsilon_0}$ is the impedance of vacuum, k_0 is the wave vector in vacuum, and β_i is the propagation constant of the ith mode. The field in the waveguides can be expanded as

$$\Psi(x,y,z,t) = \mathrm{Re}\left[\left(a_s(z)\Psi_{0s}(x,y)e^{-j\beta_{0s}z} + a_a(z)\Psi_{0a}(x,y)e^{-j\beta_{0a}z}\right)e^{j\omega t}\right]. \tag{2}$$

Here ω is the optical frequency, $a_s(z)$ and $a_a(z)$ are amplitudes of symmetric and asymmetric modes, and β_{0s} and β_{0a} are their corresponding propagation constants.

When no voltage is applied to the electrode, $a_s(z)$ and $a_a(z)$ are constants along the waveguides. When a voltage is applied to the electrode, the electric field perturbs the index profile.

Eq. (2) remains valid for small fields with z-dependent mode amplitudes $a_s(z)$ and $a_a(z)$, which in general are complex. (In some places of this article we use 'amplitude' to represent the magnitude of this 'complex amplitude' and readers should not be confused.) By applying Maxwell equations and the slowly varying approximation (detailed in Appendix I), $a_s(z)$ and $a_a(z)$ are found to satisfy the following equations:

$$\frac{\partial a_s(z)}{\partial z} = -j\chi a_a(z) e^{j\Delta\beta_0 z}, \tag{3}$$

$$\frac{\partial a_a(z)}{\partial z} = -j\chi a_s(z) e^{-j\Delta\beta_0 z}, \tag{4}$$

where $\Delta\beta_0 = \beta_{0s} - \beta_{0a}$, and

$$\chi = \frac{\omega\varepsilon_0}{4} \iint \Psi_{0s}(x,y)\Delta\varepsilon_r \Psi_{0a}(x,y)\, dx\, dy, \tag{5}$$

where $\Delta\varepsilon_r$ is the change of relative dielectric constant due to the applied voltage, $\varepsilon_r = n^2$, and n is the index of refraction. The solution to Eq. (3) and (4) is given by

$$a_s(z) = e^{j\frac{\Delta\beta_0}{2}z}\left[a_s(0)\cos bz - j\,\frac{\frac{\Delta\beta_0}{2}a_s(0) + \chi a_a(0)}{b}\sin bz\right], \tag{6}$$

$$a_a(z) = e^{-j\frac{\Delta\beta_0}{2}z}\left[a_a(0)\cos bz + j\,\frac{-\chi a_s(0) + \frac{\Delta\beta_0}{2}a_a(0)}{b}\sin bz\right], \tag{7}$$

where $b = \sqrt{\frac{(\Delta\beta_0)^2}{4} + \chi^2}$.

If we define

$$\tilde{a}_s(z) = e^{-j\beta_{0s}z} a_s(z) = e^{-j\bar{\beta}_0 z} s_s(z), \tag{8}$$

$$\tilde{a}_a(z) = e^{-j\beta_{0a}z} a_a(z) = e^{-j\bar{\beta}_0 z} s_a(z), \tag{9}$$

with

$$s_s(z) = \left[a_s(0)\cos bz - j\,\frac{\frac{\Delta\beta_0}{2}a_s(0) + \chi a_a(0)}{b}\sin bz\right], \tag{10}$$

$$s_a(z) = \left[a_a(0)\cos bz + j\,\frac{-\chi a_s(0) + \frac{\Delta\beta_0}{2}a_a(0)}{b}\sin bz\right], \tag{11}$$

where $\bar{\beta}_0 = (\beta_{0s} + \beta_{0a})/2$, then the output field amplitudes in channel 1 and 2 are given by

$$a_1(z) = \frac{1}{\sqrt{2}}(\tilde{a}_s(z) - \tilde{a}_a(z)) = \frac{1}{\sqrt{2}} e^{-j\bar{\beta}_0 z}(s_s(z) - s_a(z)), \tag{12}$$

$$a_2(z) = \frac{1}{\sqrt{2}}(\tilde{a}_s(z) + \tilde{a}_a(z)) = \frac{1}{\sqrt{2}} e^{-j\bar{\beta}_0 z}(s_s(z) + s_a(z)). \tag{13}$$

If light is launched into guide 1 and the device interaction length is L, ignoring the taper coupling, the intensities in guides 1 and 2 are given by

$$I_1(L) = 1 + (\frac{\chi^2}{b^2} - 1)\ \sin^2 bL, \tag{14}$$

$$I_2(L) = \frac{\Delta\beta_0^2}{4b^2}\ \sin^2 bL. \tag{15}$$

The two switch states are defined as

(1) cross state, when $\sin^2 bL = 1$. This gives

$$bL = m\pi + \frac{\pi}{2} \qquad (m = 0, 1, 2, \dots), \tag{16}$$

in which case $I_1(L) = \chi^2/b^2,\ I_2(L) = \Delta\beta_0^2/4b^2$.

(2) bar state, when $\sin^2 bL = 0$. This implies that

$$bL = (m+1)\pi \qquad (m = 0, 1, 2, \dots), \tag{17}$$

in which case $I_1(L) = 1,\ I_2(L) = 0$.

The crosstalk values for the two states are defined by

$$\text{Crosstalk}_{\text{cross}} = 10\ \log_{10} \frac{I_1(L)}{I_1(L) + I_2(L)}, \tag{18}$$

$$\text{Crosstalk}_{\text{bar}} = 10\ \log_{10} \frac{I_2(L)}{I_1(L) + I_2(L)}. \tag{19}$$

A perfect crosstalk for the cross state can be obtained only when $\chi = 0$, which happens only for zero applied voltage. This implies that the device has to be an odd multiple of the coupling length, $L_c = \pi/\Delta\beta_0$.

The above theory is valid for both lossless and lossy waveguides. When the symmetric and antisymmetric modes have the same propagation loss, we multiply by an exponential decay term for each mode in the modal expansion in Eq. (2). Since the propagation loss of the two modes is the same, one can factor out the decay factor, with no effect on crosstalk. If a modal differential loss exists, one can add an imaginary part to $\Delta\beta_0$ to represent the modal differential loss, and $\Delta\beta_0$ becomes complex. The solution to the coupled mode equations is still valid with complex $\Delta\beta_0$.

From Eq. (14) and (15) one can see that the coupled mode variable $2b$ can be viewed as the difference in propagation constants $\Delta\beta = \beta_s - \beta_a$ of the two waveguide eigenmodes when voltage is applied. Here subscripts 's' and 'a' denote two eigenmodes, although they are no longer symmetric and antisymmetric when voltage is applied. In the following sections, we will investigate the ideal mode expansion and see how closely $2b$ (derived from an ideal mode expansion) matches the propagation difference $\Delta\beta$ obtained through a more exact formalism.

2.2 Numerical Direct Approach to Helmholtz Wave Equation

Coupled mode theory is based upon a modal expansion into ideal symmetric and antisymmetric modes. In order to determine conditions under which this expansion is valid, we solved the Helmholtz wave equation numerically and compared the coupled mode variable $2b$ with the difference in propagation constants $\Delta\beta$ of the two eigenmodes obtained from the Helmholtz wave equation. For the sake of specificity we simulated polymer devices, but the results should be applicable to devices made of other materials such as $LiNbO_3$.

The cross section of the device with coplanar waveguide (CPW) for poling and drive electrodes is shown in Fig. 2. The electrical field distribution of this coplanar waveguide was obtained by approximating the charge distributions on the electrodes and integrating the product of the charge distribution and a Green function [25] [26]. Fig. 3 shows the field distributions of the x components of the CPW structure.

Channel waveguides are created by using a UV bleaching technique [27]. The index profile

of the UV bleached region was calculated with a model based upon a local photochemical reaction and the Kramers-Krönig relation [28]. The push-pull poling lowers the drive voltage and was used in simulation. Fig. 4 shows the poling field and the drive field of the device. The poling aligns the chromophore moieties along the poling field lines, which creates an EO effect and birefringence. It increases the index of the refraction along the poling direction and decreases the index of refraction in the perpendicular directions. Typically, the index of refraction increases by 0.02 parallel to the poling field and decreases by 0.01 perpendicular to the poling field [29].

The chromophore concentration profile can be obtained by assuming the local chromophore concentration is proportional to the local absorption coefficient, which can be obtained from the UV bleaching model [28]. The drive field together with the r coefficient profile and index profile are used to calculate the change of the index of refraction profile. For a poled polymer, the change of the local index of refraction is given by:

$$\Delta n(x,y) = -\frac{n_0^3(x,y)}{2} r_{33} E_3(x,y), \tag{20}$$

where the subscript '3' represents a direction parallel to the poling field, n_0 is the index of refraction with no field applied, r_{33} is the EO coefficient, and E_3 is the electric field component along the direction 3. For the CPW device a TE mode is assumed.

The scalar Helmholtz wave equation,

$$\nabla_t^2 \varphi(x,y) + [k_0^2 n_\varepsilon^2(x,y) - \beta^2]\varphi(x,y) = 0, \tag{21}$$

was solved numerically using the matrix effective refractive index (MERI) method [26]. Here $\varphi(x,y)$ is the transverse modal field distribution, β is the propagation constant of the mode, $n_e(x,y) = n_{e0}(x,y) + \Delta n(x,y)$ is the index profile, $n_{e0}(x,y)$ is the index profile at zero voltage and k_0 is the wave vector in vacuum. The details of solving the equation have been reported elsewhere [26].

2.3 Comparison between Coupled Mode Theory and Numerical Solution

We assume the device length is one coupling length so that the zero voltage state is the cross state, and we ignore taper coupling. The switching voltage V_0 is obtained with $m = 0$, and $b = \Delta\beta_0/2$ in Eq. (16) and $b = \sqrt{\frac{(\Delta\beta_0)^2}{4} + \chi^2(V_0)}$ in Eq. (17). V_0 should satisfy $\chi(V_0) = \frac{\sqrt{3}}{2}\Delta\beta_0$. In Fig. 5 the modal field profiles obtained from ideal mode expansion in the coupled mode theory (dashed lines) are plotted together with the field profiles calculated with numerical direct approach (solid lines) at different drive voltages. At $V = V_0$, there is almost no deviation between eigenmodes of the device calculated using the Helmholtz equation and ideal mode expansion. Non-negligible deviation starts to appear at $V = 2.3V_0$. The deviation becomes significant at $V = 4.6V_0$. Beyond $V = 7.4V_0$, one channel becomes antiguiding and the other channel becomes multimode. The ideal mode expansion is invalid for a voltage greater than $V = 3V_0$. Fig. 6 compares the propagation constant difference $\Delta\beta$ of two eigen modes calculated using the Helmholtz equation and $2b$ calculated using the coupled mode theory. $\Delta\beta$ and $2b$ are close enough to be considered equal even for a voltage five times higher than the typical drive voltage. Beyond this point, the ideal mode expansion breaks down, and $\Delta\beta$ and $2b$ separate, although the ideal mode expansion breaks down at a much lower voltage.

Simulation of a device with the coplanar-strips (CPS) electrode structure showed similar results. With the validity of the coupled mode equations verified in two different electrode configurations, they are used for calculating the propagation of the modes in the remainder of the article.

3 One-Electrode Directional Coupler and Defect Scattering Induced Crosstalk Model

Fig. 1 shows a conventional one-electrode directional coupler. A Poincaré sphere representation of the propagation and coupling of modes in a directional coupler [24] [30] is employed.

Stokes parameters are defined as follows,

$$S0 = \tilde{a}_s\tilde{a}_s^* + \tilde{a}_a\tilde{a}_a^* = \sqrt{S1^2 + S2^2 + S3^2} \tag{22}$$

$$S1 = \tilde{a}_s\tilde{a}_s^* - \tilde{a}_a\tilde{a}_a^* \tag{23}$$

$$S2 = \tilde{a}_s\tilde{a}_a^* + \tilde{a}_a\tilde{a}_s^* \tag{24}$$

$$S3 = (\tilde{a}_s\tilde{a}_a^* - \tilde{a}_a\tilde{a}_s^*)/i \tag{25}$$

$S0$ is the total power in the guides which has been normalized to one (assuming waveguides are lossless) and $S1$ is the power difference in the two modes. Using $P_s = \tilde{a}_s\tilde{a}_s^*$ and $P_a = \tilde{a}_a\tilde{a}_a^*$ to represent the powers in the symmetric and antisymmetric modes respectively, then

$$S0 = P_s + P_a, \tag{26}$$

$$S1 = P_s - P_a. \tag{27}$$

In the absence of an applied voltage and ignoring any coupling in the taper region, light launched into guide 1 excites the symmetric and antisymmetric modes equally. At the input of the interaction region of the directional coupler $z = 0$, $\tilde{a}_s = -\tilde{a}_a$, two modes have equal amplitudes and are out of phase by π. Thus, $S1 = S3 = 0$ and $S2 = 1$, as shown in Fig. 7. As the light propagates through the coupler, the state vector rotates about the $S1$ axis, tracing out a great circle in the $S2 - S3$ plane (thick solid line in Fig. 7). If at the end of the interaction length $z = L$ the state vector is at $S2 = 1$, then light is in guide 1 (a bar state), and if the state vector is at $S2 = -1$, then light is in guide 2 (a cross state).

When a voltage is applied to the electrode (so $\chi \neq 0$), the state vector rotates about a new vector in the $S1 - S2$ plane, which makes an angle α with the $S1$ axis (thick dashed line in Fig. 7), where $\tan\alpha = 2\chi/\Delta\beta_0$. The trajectory of the state vector is then no longer a great circle, but a circle still passes through $S2 = 1$, at which the coupler will be in a bar state if the interaction region ends.

As is seen in Fig. 7, a one-electrode directional coupler cannot be tuned to a cross state using any value of voltage if the device length is incorrect, since for a one-electrode directional coupler, the perfect cross state only exists at zero voltage. The crosstalk is determined by how

far the device length differs from an odd multiple of the coupling length. The device can be tuned to a bar state by applying a voltage determined from Eq. (17).

Defects perturb the modal coupling by scattering light (with a phase delay) into a specific radiation pattern which depends on the scattering mechanism. The proportion ρ of scattered light which is recaptured by the waveguides is determined by the numerical aperture (NA) of the guides through

$$\rho = \frac{\int_{NA} P(\Omega) d\Omega}{\int_{4\pi} P(\Omega) d\Omega}, \tag{28}$$

where $P(\Omega)$ is the differential radiation power in the direction Ω and subscript 'NA' represents the numerical aperture of the guide. The larger the NA, the more scattered light is recaptured, which means that stronger guides will have larger crosstalk due to scattering. The captured light re-excites the waveguide modes and propagates through the remainder of the guide. There is still a small chance for the light to be re-scattered, but it is negligible. At the output end of the interaction region, the scattered light that is captured will add coherently and interfere with the unscattered light.

In the interaction region of a directional coupler, the captured light re-excites the symmetric and antisymmetric modes. The evolution of the phase and amplitude of the two modes can be obtained from the coupled mode equations. For a given input light power, the total scattered-light power of the guide can be calculated using the scattering loss of the device. For a guide with $NA = 0.12$, assuming the differential scattering power $P(\Omega) \propto \cos^2\theta$, less than 1% of the scattered light can be recaptured. All calculations are corrected for an input power of 1 mW at a wavelength of 1.55 μm with scattering loss 0.5 dB/cm. 50,000 scattering sites were used in the simulation for each device, which were large enough to give low statistical noise.

In order to match the 0.5 dB loss in the device, the total scattered power, which is the sum of the scattered power from 50,000 scattering sites, was assumed to be 0.11 mW. The scattering sites were selected using a random number generater. They were uniformly distributed in both waveguides. The scattering sites were selected independently for each coupler simulated to approximate the randomly distributed defects in fabricated devices.

There are two kinds of excitations of the symmetric and antisymmetric modes for captured

scattered light. If the scattering is in guide 1, the phase difference between the two normal modes of the recaptured light is π. If the scattering is in guide 2, the phase difference of the two normal.modes is zero. The sum of complex amplitudes of the scattered light at $z = L$ is a random phasor sum with the phases of the recaptured light uniformly distributed between 0 and 2π due to the phase randomization of scattering [31]. It adds up coherently with the unscattered light. When light is launched into guide 1 of a coupler which is one coupling length long, unscattered light crosses to guide 2 completely if no voltage is applied. Only scattered light is present in guide 1. Its amplitude is non-zero since it is a random phasor sum. The magnitude of a random phasor sum can be shown to satisfy a Rayleigh distribution [31] if the phases of the individual components are uniformly distributed between 0 and 2π. Therefore, the scattering from defects produces background light in the guides and results in crosstalk in a directional coupler switch.

If we assume that N scattering events are involved in the scattering, light out of guide 1 is given by

$$I_1(L) = \left| \frac{\tilde{a}_s(L)e^{-\alpha_s L} - \tilde{a}_a(L)e^{-\alpha_a L}}{\sqrt{2}} + \sum_{i=1}^{N} \frac{s_s^{(i)}(L^{(i)}) - s_a^{(i)}(L^{(i)})}{\sqrt{2}} e^{-j\phi^{(i)}} \right|^2, \qquad (29)$$

where L is the interaction length of the coupler and $\tilde{a}_k = a_k e^{-j\beta_k z}$ ($k = s$ or a). $\tilde{a}_s$ and $\tilde{a}_a$ are the amplitudes of the symmetric and antisymmetric modes of the unscattered light, calculated using Eqs. (8) and (9), and (6) and (7), and α_s and α_a are the propagation loss coefficients for the symmetric and antisymmetric modes. $L^{(i)}$, representing the length measured from the *ith* scattering center to the end of the interaction region, is a random variable drawing from a uniform distribution between 0 and L. $s_s^{(i)}$ and $s_a^{(i)}$ are calculated from Eqs. (10) and Eq. (11), with the origin of the coordinates shifted to the scattering site and initial conditions $a_s(0) = -a_a(0) = \epsilon$ for scattering from guide 1, and $a_s(0) = a_a(0) = \epsilon$ for scattering from guide 2. ϵ is a constant which is adjusted to make the device loss equal to a specified scattering loss. For simulations, we used $\phi^{(i)} = \bar{\beta}_0 L^{(i)}$, which is varying rapidly enough to be equivalent to a random phase at *ith* scattering site. Since the scatterers are uniformly distributed along the waveguides, an applied voltage to the electrode will change the evolution of the recaptured light from each scatterer. Thus the sum of the recaptured light changes both in amplitude and phase

with applied voltage. At the same time, the voltage changes both the amplitude and phase of the unscattered light, but a different way from the scattered light. If a voltage exists such that the first term and the summation term inside the absolute value sign in Eq. (29) are equal in magnitude but out of phase, there is a complete cancellation of the light in guide 1, and hence zero crosstalk.

Fig. 8(a) shows the states of 192 one-coupling-length directional couplers projected onto the $S1 - S3$ plane from negative side of the $S2$ axis. The origin represents the unperturbed cross state. Each point represents a perturbed state of a directional coupler due to random scattering. Points on the $S1$ axis correspond to couplers for which the net effect of scattering is to perturb the relative amplitude of the ideal normal modes, and not their relative phase. Points on the $S3$ axis correspond to those for which the net effect of scattering is to perturb the relative phase of the ideal normal modes, and not their relative amplitude. Three circles represent the -20 dB, -30 dB, and -40 dB crosstalk contours. Fig. 8(b) shows the histogram of crosstalk values for 192 directional couplers. The solid line is a Rayleigh distribution plotted on a linear-log scale. The standard deviation of the crosstalk as observed in 48 fabricated devices [1] is close to 20 dB.

There is only one parameter σ in the Rayleigh distribution density function,

$$f(a_1) = \frac{a_1}{\sigma^2} e^{-\frac{a_1^2}{2\sigma^2}}, \tag{30}$$

When couplers are designed to switch light from guide 1 to guide 2, this equation gives the normalized light amplitude distribution out of guide 1. Then the crosstalk is given by,

$$\text{Crosstalk}_1 = 10 \log_{10} \frac{I_1}{I_1 + I_2} = 10 \log_{10} a_1^2. \tag{31}$$

Thus the crosstalk distribution is given by,

$$g(y) = \frac{\log_e 10}{20\sigma^2} 10^{y/10} \exp[-\frac{10^{y/10}}{2\sigma^2}] \qquad (-\infty < y \leq 0), \tag{32}$$

where $y = 10 \log_{10} a_1^2$ is the crosstalk. Eq. (32) is the Rayleigh distribution density function in linear-log scale and corresponds to a crosstalk distribution of identically made untuned directional coupler switches which have only scattered light present in one of the output channels.

The shape of the curve doesn't change much with σ in our range of interest (σ ranging from 2.2×10^{-1} to 6.0×10^{-6}, corresponding to the mean crosstalk varying from -10 dB to -100 dB), only its position along the horizontal axis. This implies that the crosstalk standard deviation (in dB) for fabricated devices is similar no matter how strong the scattering is.

For a one-electrode directional coupler there is only one degree of freedom with which to tune the directional coupler to a desired state, which in general is not sufficient, since both the relative phase and the relative amplitude of the two modes are perturbed by scattering. Therefore there are two independent random variables involved, so more degrees of freedom are necessary to tune the device to zero crosstalk.

4 Two-Electrode Directional Coupler

For one-electrode directional coupler switches, the cross state can only be achieved for devices having an exact odd multiple of coupling lengths at zero voltage. This imposes a tight tolerance on the device fabrication and limits the yield of mass production. The directional coupler structure with electrode sections that have alternating voltages, the reversed-$\Delta\beta$ directional coupler [6], was first proposed and analyzed in [9]. For such a device, if the length is chosen to be longer than one coupling length, the coupler can be tuned to either cross or bar state with one voltage source [6] [9].

The switching to the cross state of a reversed-$\Delta\beta$ directional coupler is illustrated on the Poincaré sphere in Fig. 9. While the light is propagating from $z = 0$ to $z = L/2$, *i.e.*, through the first electrode (with voltage V), the state vector rotates about the vector $\vec{a}$, which makes an angle α with the $S1$ axis in the $S1 - S2$ plane. The electrode voltage is chosen so that when the light reaches the end of the first electrode, the state vector lies in the $S1 - S3$ plane. When the light propagates from $z = L/2$ to $z = L$, *i.e.*, through the second electrode (with voltage $-V$), the state vector rotates about the vector $\vec{a'}$, which makes an angle $-\alpha$ with the $S1$ axis in the $S1 - S2$ plane. At the end of the second electrode $z = L$, the state vector has evolved into $S2 = -1$, which represents the cross state. Thus with two electrode

voltages of opposite polarity, one can cancel the change in the the relative amplitude of a_s and a_a induced by applying voltages, allowing one to tune to the cross state. Two-electrode reversed-$\Delta\beta$ directional couplers have been used in 8×8 Ti:$LiNbO_3$ switches due to their high yield [23], [32].

Long term stability of directional coupler devices is required in many applications. $LiNbO_3$ optical modulators and switches often exhibit DC drift, which causes the switching voltage to vary over a long time span. Mobile charges in the SiO_2 buffer layer accumulate and perturb the applied electric field in the waveguide, inducing DC drift [10] [11] [33]. Phosphorus doping in the SiO_2 layer has been used to passivate the mobile charges and reduce DC drift [34]. Dry oxygen annealing also was found useful for reducing the DC drift [35]. The pyroelectric properties of $LiNbO_3$ can also result in charges on the surface of the crystal and produces undesired thermal drift [36]. Optical drift has also been reported due to the photorefractive effect in the $LiNbO_3$ substrate [37]. Because of these various sources of drift, $LiNbO_3$ devices need to be tuned frequently to maintain low crosstalk.

Any asymmetry between the two electrodes in reversed-$\Delta\beta$ couplers can produce crosstalk. Fabrication errors in devices introduce asymmetry in the electrode lengths, and lateral misalignment of the electrodes result in an asymmetric switching field in the waveguides. Domain reversal induced in processing can also introduce asymmetry in the two electrode sections [21]. To reduce the crosstalk due to asymmetry of the electrodes, fine tuning of reversed-$\Delta\beta$ couplers is necessary.

In order to correct for DC drift and fabrication errors, the voltages on the two electrodes have been independently adjusted to fine-tune the coupler to either the cross or bar state [12] The layout of such a switch is shown in Fig. 10.

Identically fabricated reversed-$\Delta\beta$ directional coupler switches exhibit a distribution of crosstalk values. This phenomenon can be explained by scattering as discussed in the last section. Fig. 11(a) shows the state vectors of 192 simulated couplers projected onto the $S1 - S3$ plane with identical physical design, the same applied voltages (as reversed-$\Delta\beta$ couplers), and the same number of scattering centers (50,000) but different scattering locations, which were selected by using a random number generater. Fig. 11(b) shows the crosstalk distribution.

Fig. 11 is similar to the case of passive (with zero applied electrode voltage) couplers as shown in Fig. 8.

By independently adjusting the DC biasing voltages, each device can be tuned to a desired state. In simulating $LiNbO_3$ devices with about 5 Volt switching voltage and tenths of millivolts of control accuracy, all the devices were tuned to the cross state with better than -60 dB crosstalk. With picovolts of control accuracy all the devices could achieve better than -300 dB crosstalk. The results are shown in Table 1.

On a Poincaré sphere, only two angular variables, which correspond to the relative phase and relative amplitude of the two modes, are needed to determine the state of a device. These can be controlled by two independent voltages. Therefore, two voltages are sufficient for tuning directional couplers to a desired state when only scattering is considered in the crosstalk model for realistic values of scattering loss.

However, differential loss is also a limiting factor in achieving low crosstalk. In simulation, differential loss was added in by assuming a complex $\Delta\beta_0$ in the coupled mode equations. Simulation showed that as long as the differential loss remains below 0.3 dB (for 2.5 cm long interaction length), two electrode voltages remain sufficient to tune out the crosstalk completely due to scattering and differential loss. However, when differential loss exceeds 0.5 dB, two electrode voltages were found to be insufficient to tune out the crosstalk for this geometry.

Coupling in the taper region can also increase the crosstalk [5] [15]. If the taper region only introduces a relative phase between the two coupled modes, this is equivalent to a device length error in a passive coupler, and two electrode voltages can tune out the crosstalk. If there is unequal coupling into the two modes at the input or modal conversion in the taper region due to the asymmetry of the two waveguides, there will be a difference in amplitudes of the two modes. Two longitudinally symmetric electrodes cannot tune out the crosstalk when the amplitude difference is sufficiently large. An additional electrode provides the flexibility needed to compensate for this effect.

All causes of crosstalk other than scattering and modal differential loss can be treated effectively as unequal taper coupling. Using a transfer matrix one can write the modal vector as

$$\begin{pmatrix} a_s \\ a_a \end{pmatrix} = \begin{pmatrix} e^{a+jd} & 0 \\ 0 & e^{-a-jd} \end{pmatrix} \begin{pmatrix} a_{s0} \\ a_{a0} \end{pmatrix}, \tag{33}$$

where a is called the taper asymmetry factor and d is called the phase factor, and both a and d are real numbers.

A 'realistic' crosstalk model, which combines the scattering together with differential loss and unequal coupling, was used to simulate the crosstalk tuning. Table. 2 shows the tuning of a 'realistic' directional coupler. Complete elimination of crosstalk is impossible with two electrodes for this geometry.

5 Three-Electrode Directional Coupler

Three-electrode directional couplers [1] have three independent tuning voltages and offer one more degree of freedom to minimize the crosstalk. Experimentally, Choquette and his co-workers [5] have achieved -47.8 dB for the bar state and -34.6 dB for the cross state with such a structure. Three-electrode directional couplers, as depicted in Fig. 12, were simulated with scattering loss. The total interaction length was 2.5 coupling lengths. Two voltages with the same amplitude and opposite polarity were applied to the two outer electrodes of the device to obtain a cross state. The 192 devices simulated showed a crosstalk distribution similar to the 2-electrode directional couplers. Like 2-electrode directional couplers, with tenths of millivolts of accuracy we have been able to tune all the devices to a desired state with crosstalk better than -60 dB. Picovolts of accuracy allowed for the devices to be tuned to be better than -300 dB crosstalk.

By independently adjusting the voltages on all three electrodes, tuning out crosstalk due to differential loss and scattering was simulated. The crosstalk can be tuned out completely even for the case of 10 dB/cm differential loss. Table. 3 shows the simulation results on three-electrode couplers with 'realistic' device parameters, in which the unequal coupling and the taper coupling and differential loss were taken into account together with scattering, and better

than -100 dB crosstalk can be achieved.

6 Discussion

Compared to the random index perturbation model used in analyzing $LiNbO_3$ couplers, the scattering induced crosstalk model gives a better fit to the crosstalk distribution obtained from identically fabricated directional couplers [23]. Furthermore, in this model the crosstalk is calculated based on known values for the scattering loss and NA of the waveguides. The model predicts that crosstalk can be minimized by lowering the scattering loss and reducing the NA of the channel waveguides.

All crosstalk mechanisms result in random relative phase shifts and randomly unequal modal strengths ($|a_s| \neq |a_a|$). The electrode voltages also vary the relative phase shift and relative modal strengths, which with proper arrangement can compensate the relative phase shift and unequal modal strengths due to scattering, differential loss, fabrication errors, and taper coupling. This is equivalent to letting the terms within the absolute value sign of Eq. (29) cancel. With two electrodes one can tune out any relative phase shift, but there is a limit to how much unequal modal strengths can be tuned out. With three electrodes a wider range of unequal modal strengths can be compensated. Putting more electrodes on the device can improve the achievable crosstalk by providing additional flexibility to adjust the relative modal strength.

Our simulations assumed the light is 100% coherent and 100% linearly polarized (TE or TM). This assumption allows for complete cancellation of the light in a waveguide and achieving a perfect bar state or cross state. However, no light source is 100% coherent or 100% polarized in a certain direction. Typically, the polarization extinction can be controlled to no better than 60 dB, which will limit the cancellation of the light and result in crosstalk. There is also a depolarization effect due to scattering, although the depolarization effect is a second order (20 dB down) with respect to the capturing of the light in the same polarization as the exciting light. Furthermore, any real detector has a minimum detectable power, which implies

a limit to how well crosstalk can be tuned out. For existing technology with the best control of the polarization and coherence of light, with 0.1 dB/cm scattering loss in the waveguides, the achievable crosstalk limit is estimated to be no better than -60 dB.

7 Conclusions

Simulation of active directional couplers using a scattering-induced crosstalk model in the absence of tuning shows a Rayleigh distribution of crosstalk values. To achieve low crosstalk passively, low scattering loss and small NA waveguides are essential. The scattering-induced crosstalk can be tuned out with only two electrodes. Three electrodes are needed to tune the device back to a desired state for realistic device parameters, in agreement with experiment [1]. The practical achievable crosstalk in a directional coupler switch is no better than -60 dB due to finite coherence and incomplete polarization of the light source, and reasonable precision and stability for the tuning voltages. In order to reduce the crosstalk in directional couplers defects need to be reduced. Improved processing of integrated optical devices can help improve the crosstalk.

8 Appendix I

Assume the optical mode is TE polarized, so the waveguide field Ψ in Eq. (2) is the electric field, and $\vec{E} = E_x\hat{x} = \Psi\hat{x}$. Applying the Maxwell equation

$$\nabla \times \vec{E} = -\mu_0 \frac{\partial \vec{H}}{\partial t} \tag{34}$$

to Eq. (2), we have

$$H_y = (\frac{a_s}{\eta_s} + \frac{j}{\omega\mu_0}\frac{da_s}{dz})\Psi_{0s}e^{-j\beta_s z} + (\frac{a_a}{\eta_a} + \frac{j}{\omega\mu_0}\frac{da_a}{dz})\Psi_{0a}e^{-j\beta_a z}. \tag{35}$$

Substituting Eq. (2) and Eq. (35) into the Maxwell equation

$$\nabla \times \vec{H} = (\varepsilon + \Delta\varepsilon)\frac{\partial \vec{E}}{\partial t}, \tag{36}$$

and using the slow varying approximation

$$\left|\frac{d^2 a_s}{dz^2}\right| \ll \left|\beta_s \frac{da_s}{dz}\right|, \tag{37}$$

$$\left|\frac{d^2 a_a}{dz^2}\right| \ll \left|\beta_a \frac{da_a}{dz}\right|, \tag{38}$$

we obtain

$$\beta_s \frac{da_s}{dz}\Psi_{0s}e^{-j\beta_s z} + \beta_a \frac{da_a}{dz}\Psi_{0a}e^{-j\beta_a z} = -\frac{jk_0^2\Delta\varepsilon_r}{2}(a_s\Psi_{0s}e^{-j\beta_s z} + a_a\Psi_{0a}e^{-j\beta_a z}). \tag{39}$$

Multiplying Eq. (39) by Ψ_s or Ψ_a and integrating over the cross section we obtain

$$\frac{\partial a_s(z)}{\partial z} = -j(\chi_{ss}a_s(z) + \chi_{sa}a_a(z)e^{j\Delta\beta_0 z}), \tag{40}$$

$$\frac{\partial a_a(z)}{\partial z} = -j(\chi_{aa}a_a(z) + \chi_{as}a_s(z)e^{-j\Delta\beta_0 z}), \tag{41}$$

where

$$\chi_{pq} = \frac{\omega\varepsilon_0}{4}\iint \Psi_{0p}(x,y)\Delta\varepsilon_r\Psi_{0q}(x,y)\,dx\,dy, \tag{42}$$

and $p, q = s, a$.

Assuming the perturbation $\Delta\varepsilon$ is antisymmetric, therefore, $\chi_{ss} = \chi_{aa} = 0$ and $\chi_{sa} = \chi_{as} = \chi$ we obtain Eq. (3) and Eq. (4).

References

[1] L. McCaughan and S. K. Korotky, "Three-electrode Ti:$LiNbO_3$ optical switch," *IEEE J. Lightwave Technol.*, vol. LT-4, pp. 1324–1327, 1986.

[2] H. A. Haus, N. A. Whitaker, and Jr., "Elimination of cross talk in optical directional couplers," *Appl. Phys. Lett*, vol. 46, pp. 1–3, 1985.

[3] D. Li, "Elimination of crosstalk in directional coupler switches," *Opt. Quantum Electron.*, vol. 25, pp. 255–260, 1993.

[4] L. McCaughan and K. D. Choquette, "Crosstalk in Ti:$LiNbO_3$ directional coupler switches caused by Ti concentration fluctuations," *IEEE J. Quantum Electron.*, vol. QE-22, pp. 947–951, 1986.

[5] K. D. Choquette, L. McCaughan, and W. K. Smith, "Improved optical switching extinction in three-electrode Ti:$LiNbO_3$ directional couplers," *Appl. Phys. Lett.*, vol. 25, pp. 2097–2099, 1987.

[6] T. Findakly and F. J. Leonberger, "On the crosstalk of reversed-$\Delta\beta$ directional coupler switches," *IEEE J. Lightwave Technol.*, vol. LT-6, pp. 36–40, 1988.

[7] H. Mak and H. Tanagawa, "High-extinction directional coupler switches by compensation and elimination methods," *IEEE, J. Lightwave Technol.*, vol. 12, pp. 899–908, 1994.

[8] R. C. Alferness, "Guided-wave devices for optical communication," *IEEE J. Quantum Electron.*, vol. QE-17, pp. 946–959, 1981.

[9] H. Kogelnik and R. V. Schmidt, "Switched directional couplers with alternating $\Delta\beta$," *IEEE J. Quantum Electron.*, vol. QE-12, pp. 396–401, 1976.

[10] S. Yamada and M. Minakata, "DC drift phenomena in $LiNbO_3$ optical waveguide devices," *Jpn. J. Appl. Phys.*, vol. 20, pp. 733–737, 1981.

[11] C. M. Gee, G. D. Thurmond, H. Blauvelt, and H. W. Yen, "Minimizing DC drift in $LiNbO_3$ waveguide devices," *Appl. Phys. Lett.*, vol. 47, pp. 211–213, 1985.

[12] F. T. Stone, J. E. Watson, D. T. Moser, and W. J. Minford, "Performance and yield of pilot-line quantities of lithium niobate switches," in *Proc. SPIE*, Vol. 1177, 1989, pp. 322–326.

[13] R. V. Schmidt and H. Kogelnik, "Electro-optically switched coupler with stepped $\Delta\beta$ reversal using Ti-diffused $LiNbO_3$ waveguides," *Appl. Phys. Lett.*, vol. 28, pp. 503–505, 1976.

[14] S. Lin, W. Feng, R. B. Hooker, and A. R. Mickelson, "UV bleaching of polymers and polymeric directional couplers for optical interconnects," in G. R. Möhlman, ed., (*Proc. SPIE*), Vol. 2285, 1994, pp. 415–423.

[15] S. Thaniyavarn, "Cross-talk characteristics of $\Delta\beta$ phase reversal directional coupler switches," in *Proc. SPIE*, Vol. 578, 1985, pp. 192–198.

[16] J. Weber, L. Thylén, and S. Wang, "Crosstalk and switching characteristics in directional couplers," *IEEE J. Quantum Electron.*, vol. 24, pp. 537–548, 1988.

[17] K. Chen and S. Wang, "Cross-talk problems in optical directional couplers," *Appl. Phys. Lett.*, vol. 44, pp. 166–168, 1984.

[18] D. Marcuse, *Light Transmission Optics.* New York: Van Nostand Reinhold, 1972.

[19] V. R. Chinni, T. C. Huang, P. K. Wai, C. R. Menyuk, and G. J. Simonis, "Crosstalk in a lossy directional coupler switch," *IEEE J. Lightwave Technol.*, vol. 13, pp. 1530–1535, 1995.

[20] L. McCaughan and K. D. Choquette, "Ti-concentration inhomogeneities in Ti:$LiNbO_3$ waveguides," *Opt. Lett.*, vol. 12, pp. 567–569, 1987.

[21] S. Thaniyavarn, T. Findakly, D. Booher, and J. Moen, "Domain inversion effects in Ti-$LiNbO_3$ integrated optical devices," *Appl. Phys. Lett.*, vol. 46, pp. 933–935, 1985.

[22] A. J. Weierholt, A. R. Mickelson, and S. Neegard, "Eigenmode analysis of symmetric parallel waveguide coupler," *IEEE J. Quantum Electron.*, vol. 12, pp. 1689–1700, 1987.

[23] J. E. Watson, M. A. Milbrodt, K. Bahadori, M. F. Dautartas, C. T. Kemmerer, D. T. Moser, A. W. Schelling, T. O. Murphy, J. J. Veselka, and D. A. Herr, "A low-voltage 8×8 Ti:$LiNbO_3$ switch with a dilated-benes architecture," *J. Lightwave Technol.*, vol. 8, pp. 794–800, 1990.

[24] S. K. Korotky, "Three-space representation of phase- mismatch switching in coupled two-state optical systems," *IEEE J. Quantum Electron.*, vol. QE-22, pp. 952–958, 1986.

[25] P. S. Weitzman, "Evaluation of electric field distributions and capacitance of electrode structures used in intergrated optic modulators," Guided Wave Optics Laboratory Rep. 16, ECE Dept., Univ. of Colorado at Boulder, 1990.

[26] W. Charczenko, P. S. Weitzman, H. Klotz, M. Surette, J. M. Dunn, and A. R. Mickelson, "Characterization and simulation of proton exchanged integrated optical modulators with various dielectric buffer layers," *J. Lightwave Technol.*, vol. LT-9, pp. 92–100, 1991.

[27] M. B. J. Diemeer, F. M. M. Suyten, E. S. Trommel, A. McDonach, J. M. Land, L. W. Jenneskens, and W. H. G. Horsthuis, "Photoinduced channel waveguide formation in nonlinear optical polymers," *Electron. Lett.*, vol. 26, pp. 379–380, 1990.

[28] J. Ma, S. Lin, W. Feng, R. J. Feurstein, R. B. Hooker, and A. R. Mickelson, "Modeling photobleached optical polymer waveguides," *Appl. Opt.*, vol. 34, pp. 5352–5360, 1995.

[29] M. Eich, A. Sen, H. Looser, G. C. Bjorklund, J. D. Swalen, R. J. Twieg, and D. Y. Yoon, "Corona poling and real time second-harmonic generation study of a novel covalently functionalized amorphous nonlinear optical polymer," *J. Appl. Phys.*, vol. 66, pp. 2559–2567, 1989.

[30] B. Daino, G. Gregori, and S. Wabnitz, "Stability analysis of nonlinear coherent coupling," *J. Appl. Phys.*, vol. 58, pp. 4512–4514, 1985.

[31] J. W. Goodman, *Statistical Optics.* New York: John Wiley & Sons, 1985.

[32] E. J. Murphy, C. T. Kemmerer, D. T. Moser, M. R. Surbin, J. E. Watson, and P. L. Stoddard, "Uniform 8×8 lithium niobate switch arrays," *J. Lightwave Technol.*, vol. 13, pp. 967 – 970, 1995.

[33] G. L. Tangonan, D. L. Persechini, J. F. Lotseich, and M. K. Barnoski, "Electro-optic diffraction modulation in Ti-diffused $LiNbO_3$," *Appl. Opt.*, vol. 17, pp. 3259–3263, 1978.

[34] T. Suhara, M. Fujimura, K. Kinoshita, and H. Nishihara, "Reduction of DC drift in $LiNbO_3$ waveguide electro-optic devices by phosphorus doping in SiO_2 buffer layer," *Electron. Lett.*, vol. 26, pp. 1409–1410, 1990.

[35] H. Nagata, J. Ichikawa, M. Kobayashi, J. Hidaka, H. H. da, K. Kiuchi, and T. Sugamata, "Possibility of dc drift reduction of Ti:$LiNbO_3$ modulators via dry O_2 annealing process," *Appl. Phys. Lett.*, vol. 64, pp. 1180–1182, 1994.

[36] P. Skeath, C. H. Bulmer, S. C. Hiser, and W. K. Burns, "Novel electrostatic mechanism in the thermal instability of Z-cut $LiNbO_3$ interferometers," *Appl. Phys. Lett.*, vol. 49, pp. 1221–1223, 1986.

[37] T. Fujiwara, S. Sato, H. Mori, and Y. Fujii, "Suppression of crosstalk drift in Ti:$LiNbO_3$ waveguide switches," *J. Lightwave Technol.*, vol. LT-6, pp. 909–915, 1988.

Table 1: Two-voltage tuning of scattering induced crosstalk

	V1(V)	V2(V)	Crosstalk(dB)
Untuned	6.1575	-6.1575	-25.9
Tune1	5.6632	-6.0540	<-60dB
Tune2	5.669079608421	-5.604156263459	<-300dB

Table 2: Two-voltage tuning of 'realistic' crosstalk

Modal Differential Loss (dB)	Taper Asymmetry* Factor	Taper Phase (Degrees)	Tuned Crosstalk (dB)
0.02	0.01	5.7	-43.1
0.03	0.02	5.7	-35.2
0.05	0.02	5.7	-22.6

* Taper Asymmetry is a in Eq. (33).

Table 3: Three-voltage tuning of 'realistic' crosstalk

Modal Differential Loss (dB)	Taper Asymmetry Factor	Taper Phase (Degrees)	Tuned Crosstalk (dB)
0.1	0.04	5.7	<-100
0.5	0.1	11.4	<-100

9 Figure Captions

Fig. 1 Layout of an one-electrode directional coupler.

Fig. 2 Cross section of a polymeric directional coupler with CPW poling/drive electrodes.

Fig. 3 X-component of the electric field under the CPW electrodes when unit voltage is applied on the center conductor of the electrodes.

Fig. 4 Illustration of (a) poling field and (b) drive field in the polymer waveguides.

Fig. 5 Modal field profiles at different drive voltages obtained from direct approach to the Helmholtz wave equation (solid lines) and ideal mode expansion used in coupled mode theory (dashed lines). The thicker lines represent the lowest order mode and the thinner lines represent the higher order mode.

Fig. 6 Comparison between the difference of the propagation constants of local normal modes $\Delta\beta$ and coupled mode theory variable $2b$ at different drive voltages.

Fig. 7 Illustration of the state vector evolution in one-electrode directional coupler at zero voltage (thick solid line) and voltage V (thick dashed line) on the Poincaré sphere.

Fig. 8 (a) The projection of the states of 192 one-coupling length directional couplers on the $S1-S3$ plane from negative $S2$ side. (b) The crosstalk histogram of the 192 directional couplers. The dashed line is a Rayleigh distribution function plotted in linear-log scale.

Fig. 9 Illustration of the state vector evolution in two-electrode reversed-$\Delta\beta$ directional coupler. (a) 3D view and (b) projection from 'north pole' on $S1 - S2$ plane. The layout of the two-electrode reversed-$\Delta\beta$ directional coupler is the same as in Fig. 10 (b) with $V1 = +V$, $V2 = -V$, $L1 = L2$, $L = L1 + L2 = 2.5L_c$.

Fig. 10 (a) Layout of the reversed-$\Delta\beta$ directional coupler with two DC bias voltages for fine-tuning of crosstalk, after reference [12] which is equivalent to a two-electrode directional coupler as in (b) with $V1 = V - V1(\text{Bias})$, $V2 = -V + V2(\text{Bias})$. V is switching voltage of the reversed-$\Delta\beta$ directional coupler.

Fig. 11 (a) The projection of the cross states of 192 untuned reversed-$\Delta\beta$ directional couplers

on the $S1 - S3$ plane from negative $S2$ side. (b) The crosstalk histogram of the 192 directional couplers. The dashed line is a Rayleigh distribution function plotted in linear-log scale.

Fig. 12 Layout of a three-electrode directional coupler. $L = L1 + L2 + L3 = 2.5L_c$, $L1 : L2 : L3 = 3 : 4 : 3$.

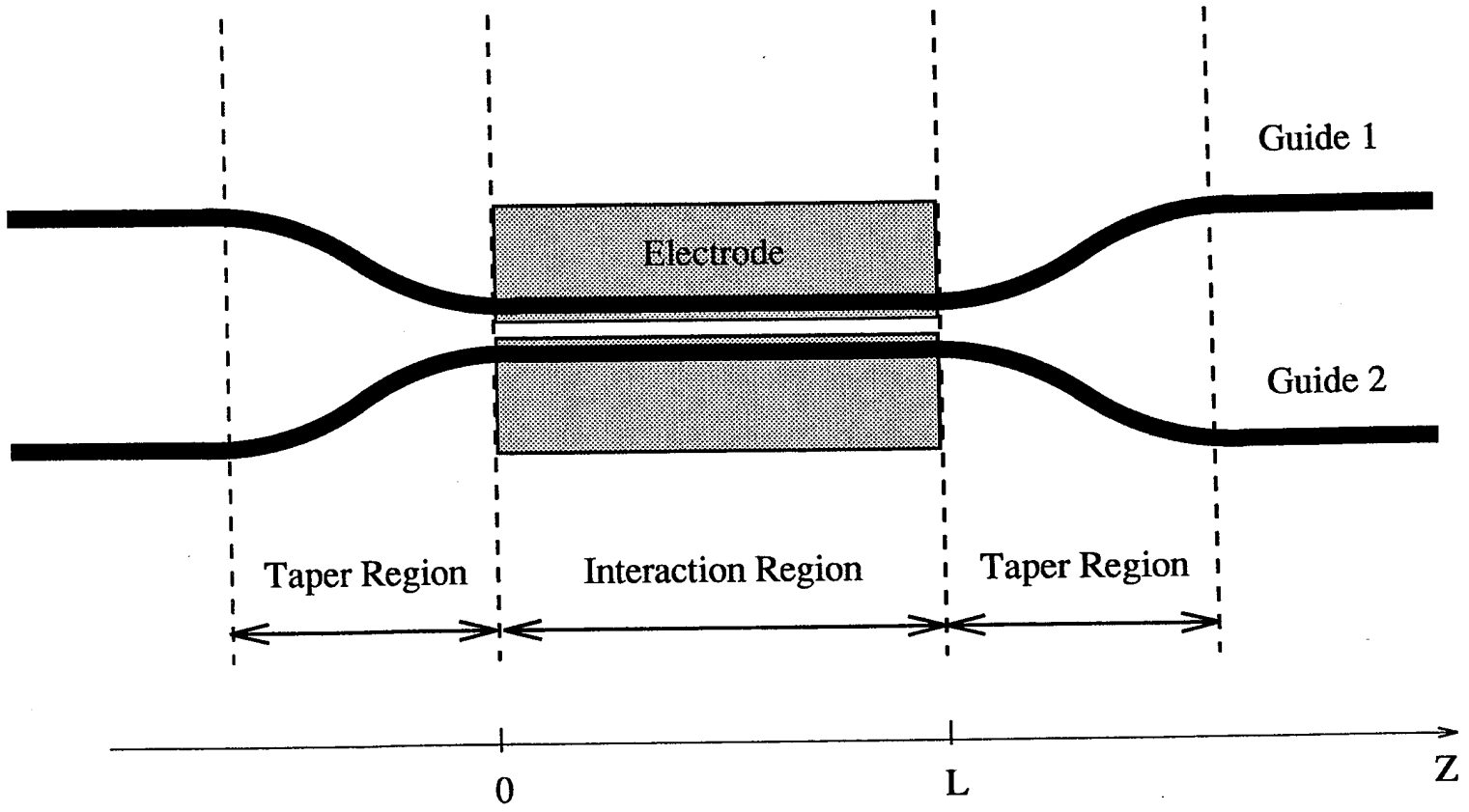
Guide 1
Electrode
Guide 2
Taper Region
Interaction Region
Taper Region
0
L
Z

Fig. 1

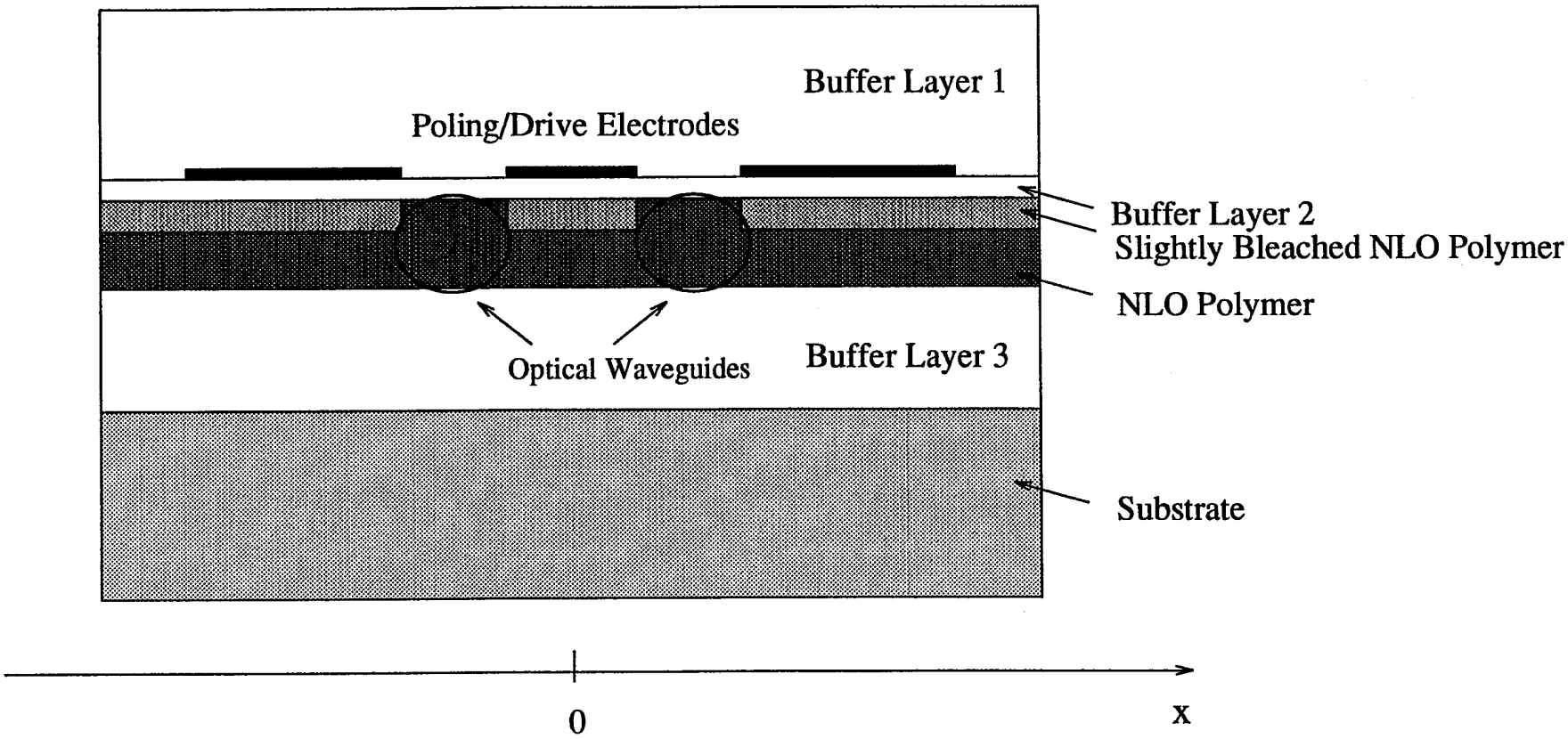
Buffer Layer 1
Poling/Drive Electrodes
Buffer Layer 2
Slightly Bleached NLO Polymer
NLO Polymer
Optical Waveguides
Buffer Layer 3
Substrate
0
x

Fig. 2

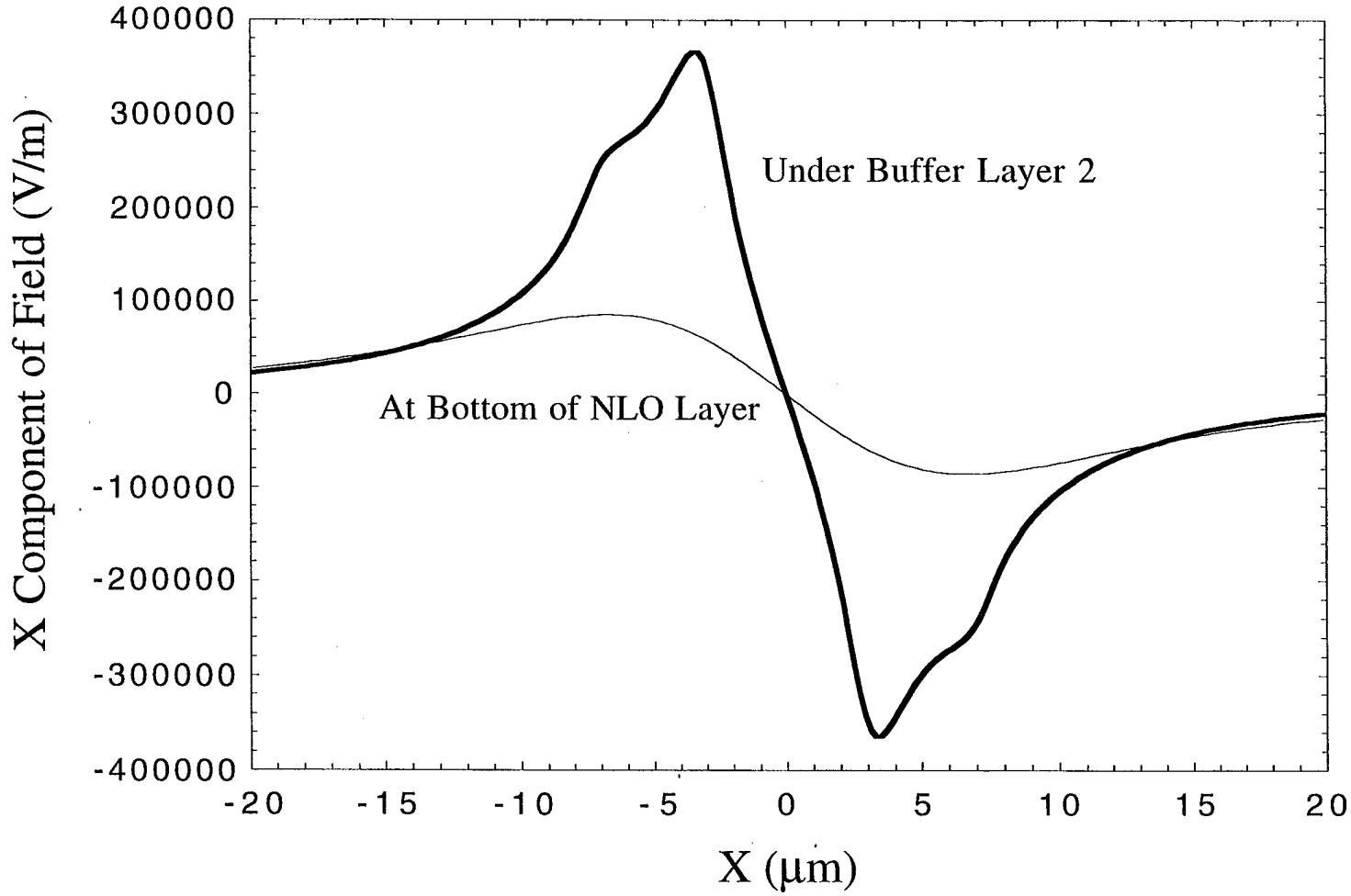
400000
300000
200000
100000
0
-100000
-200000
-300000
-400000
X Component of Field (V/m)
Under Buffer Layer 2
At Bottom of NLO Layer
-20
-15
-10
-5
0
5
10
15
20
X (μm)

Fig. 3

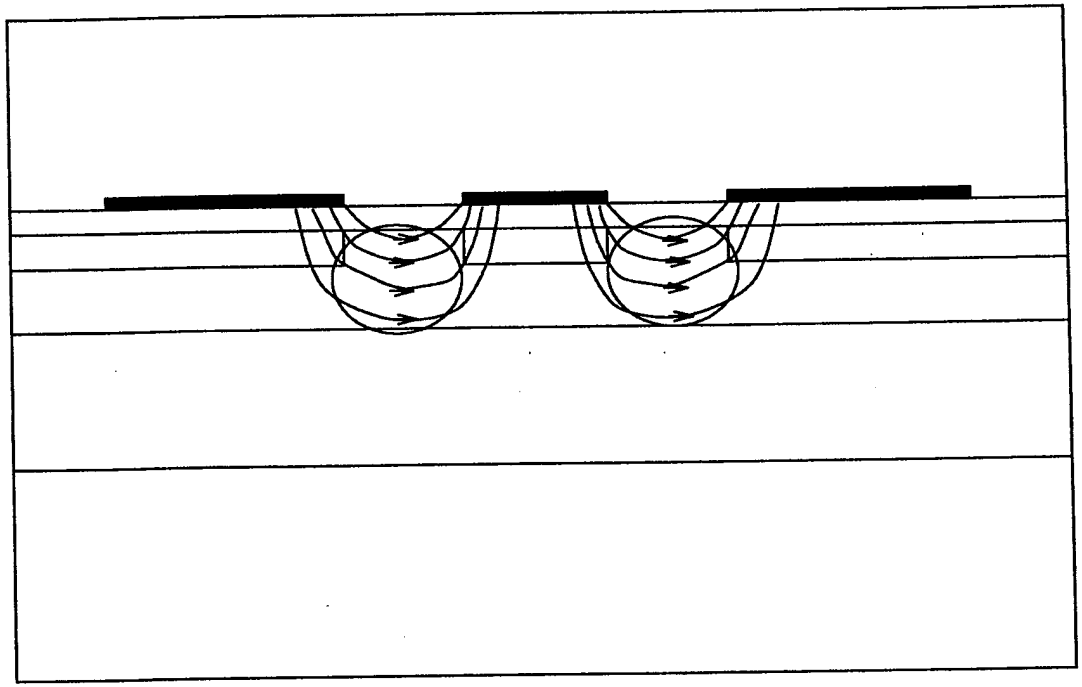

Fig. 4 (a)

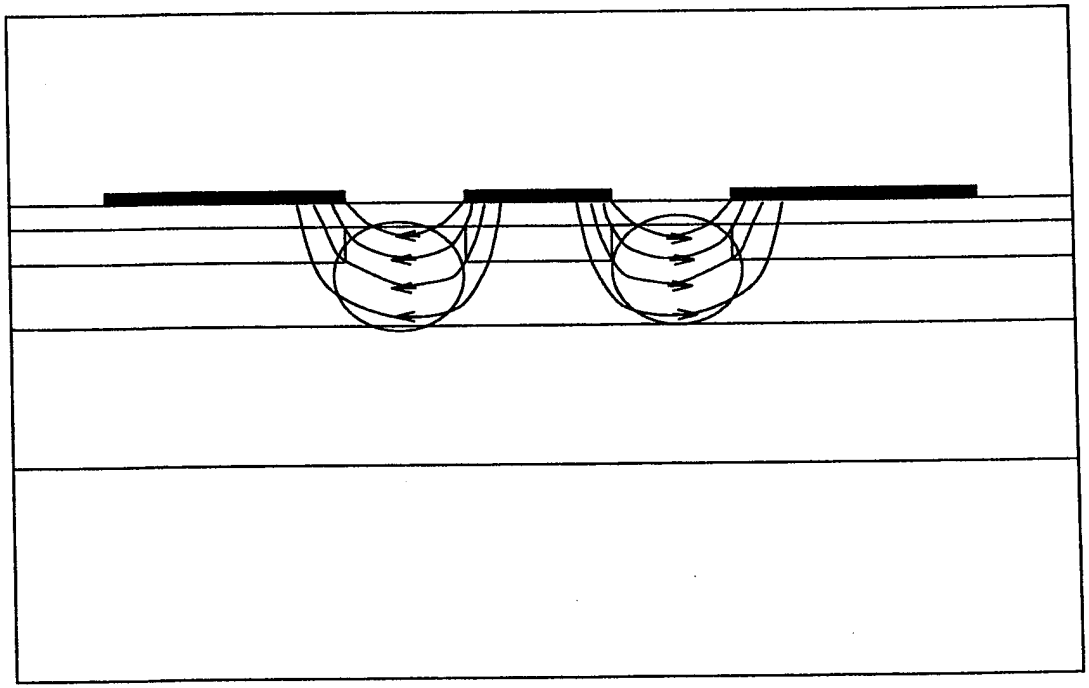

Fig. 4 (b)

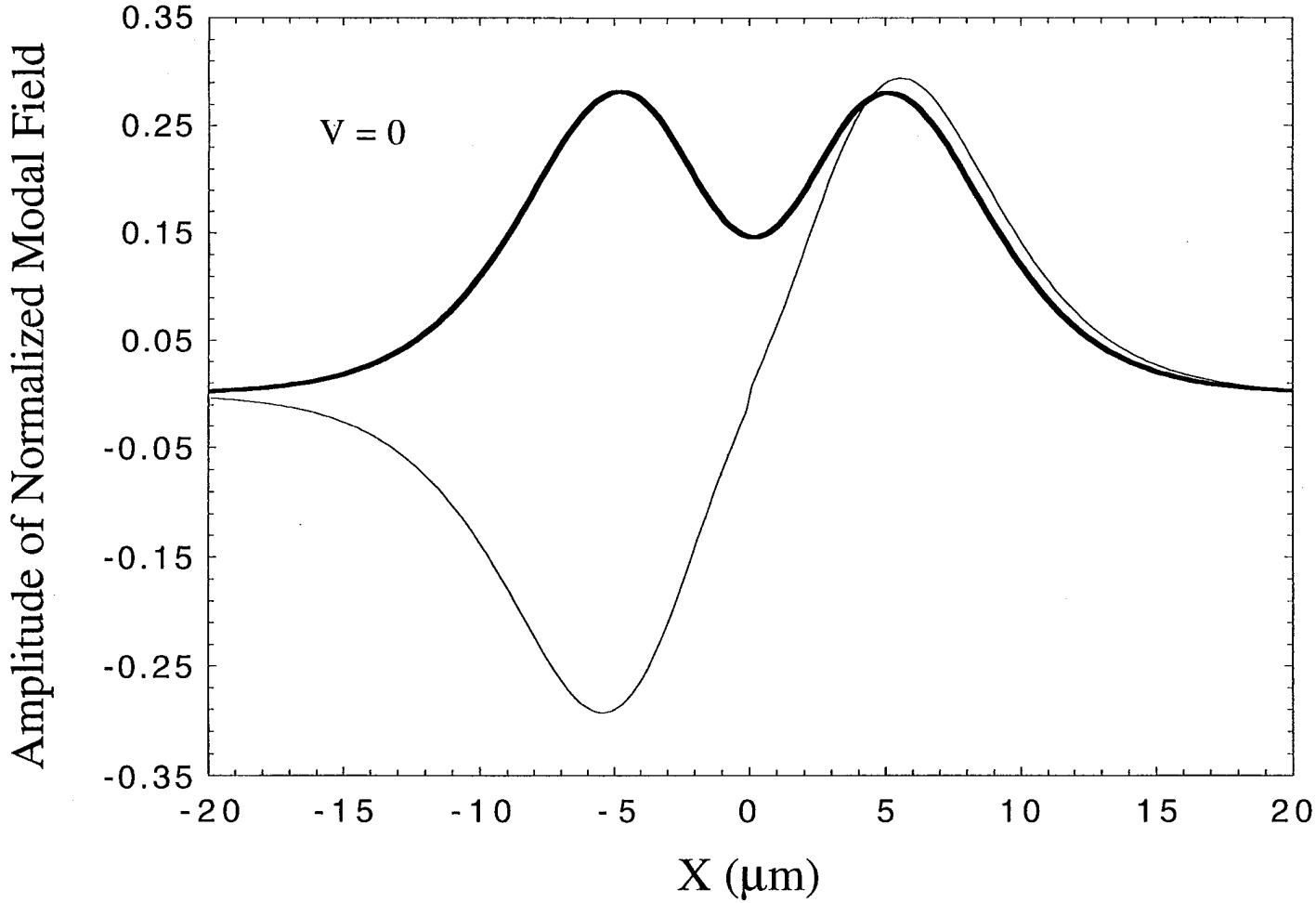
Amplitude of Normalized Modal Field
0.35
0.25
0.15
0.05
-0.05
-0.15
-0.25
-0.35
V = 0
-20
-15
-10
-5
0
5
10
15
20
X (μm)

Fig 5 (a)

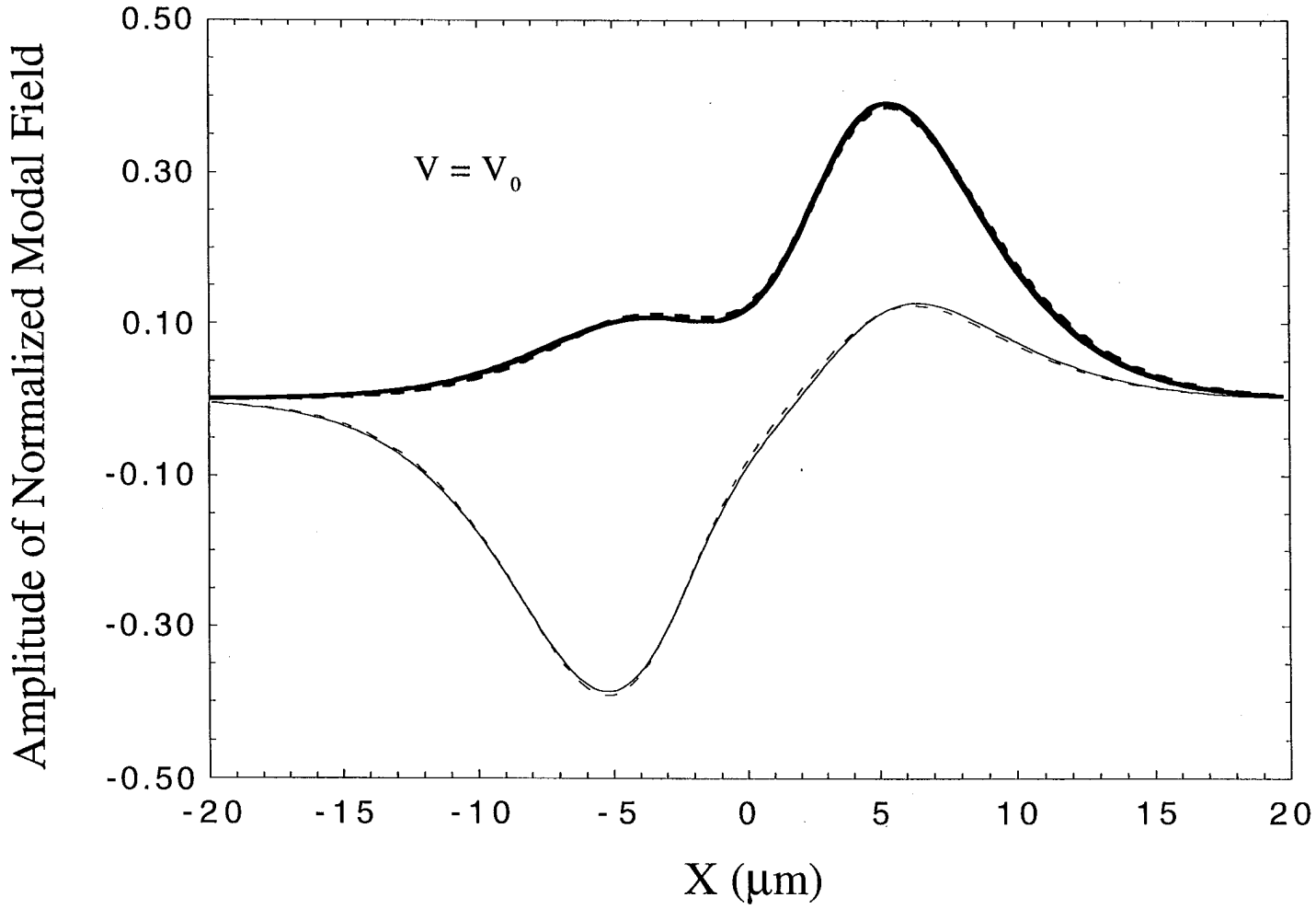
Amplitude of Normalized Modal Field
0.50
0.30
0.10
-0.10
-0.30
-0.50
V = V0
-20
-15
-10
-5
0
5
10
15
20
X (μm)

Fig 5 (b)

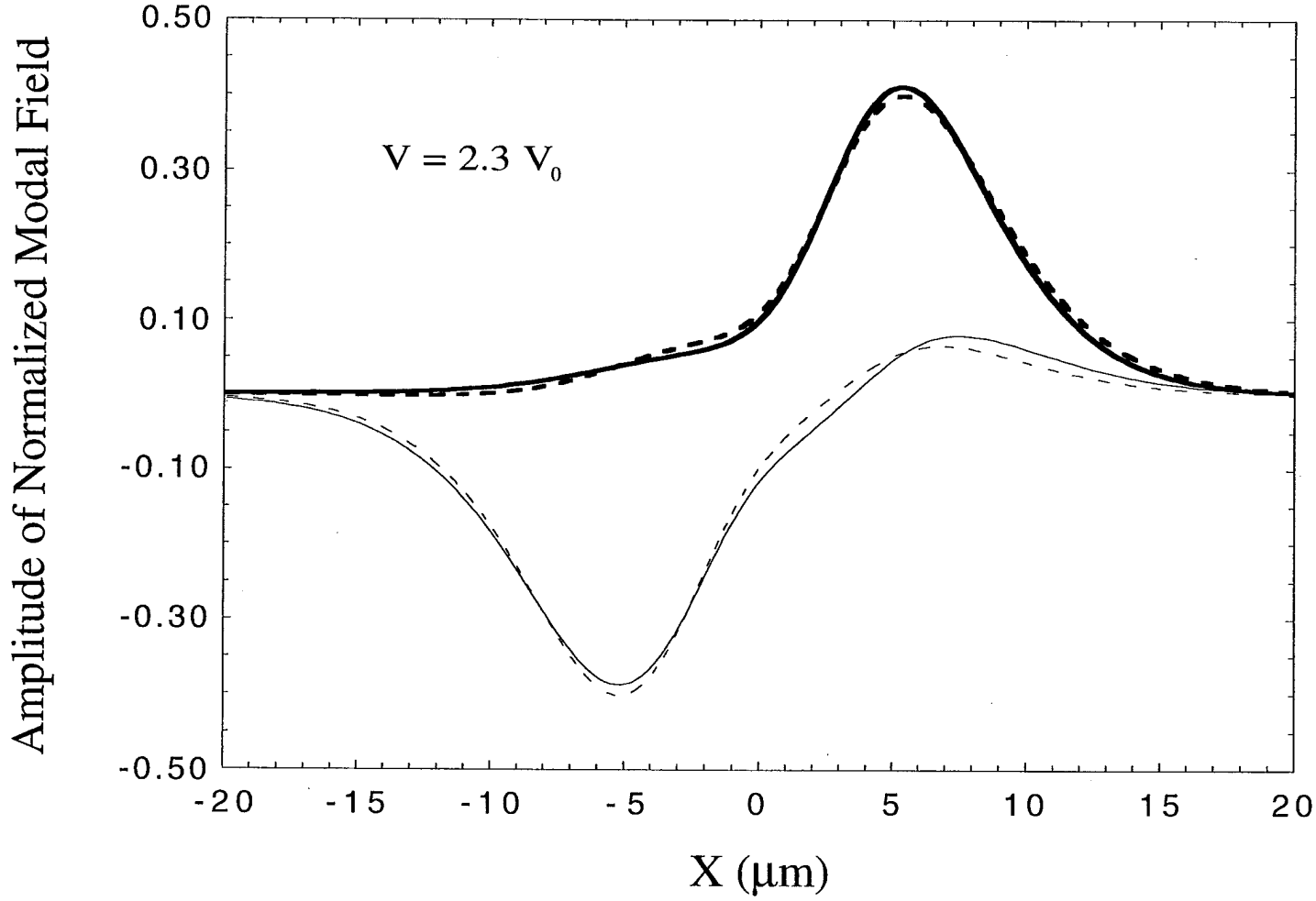
Amplitude of Normalized Modal Field
0.50
0.30
0.10
-0.10
-0.30
-0.50
V = 2.3 V0
-20
-15
-10
-5
0
5
10
15
20
X (μm)

Fig. 5 (c)

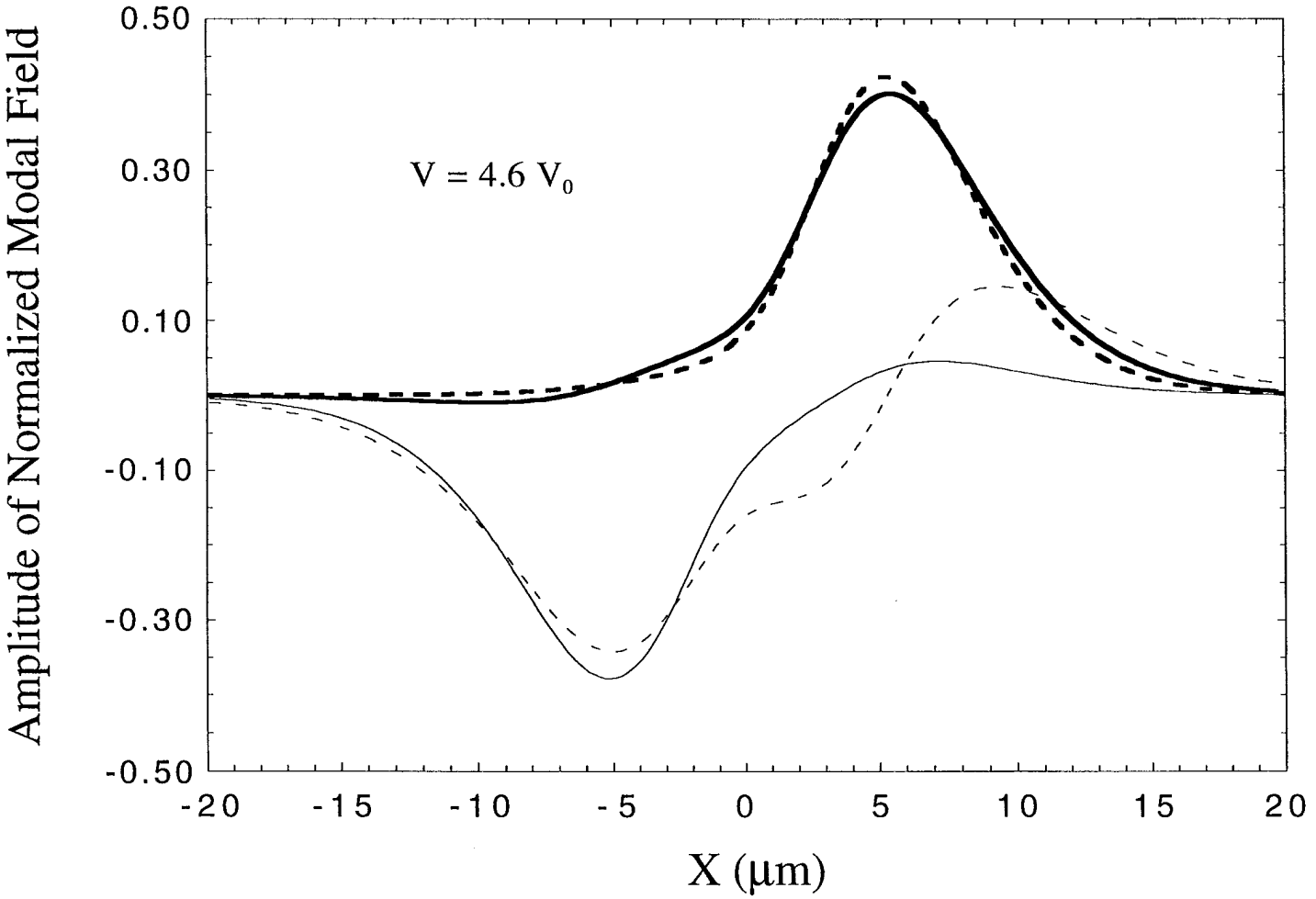
Amplitude of Normalized Modal Field
0.50
0.30
0.10
-0.10
-0.30
-0.50
V = 4.6 V0
-20
-15
-10
-5
0
5
10
15
20
X (μm)

Fig 5(d)

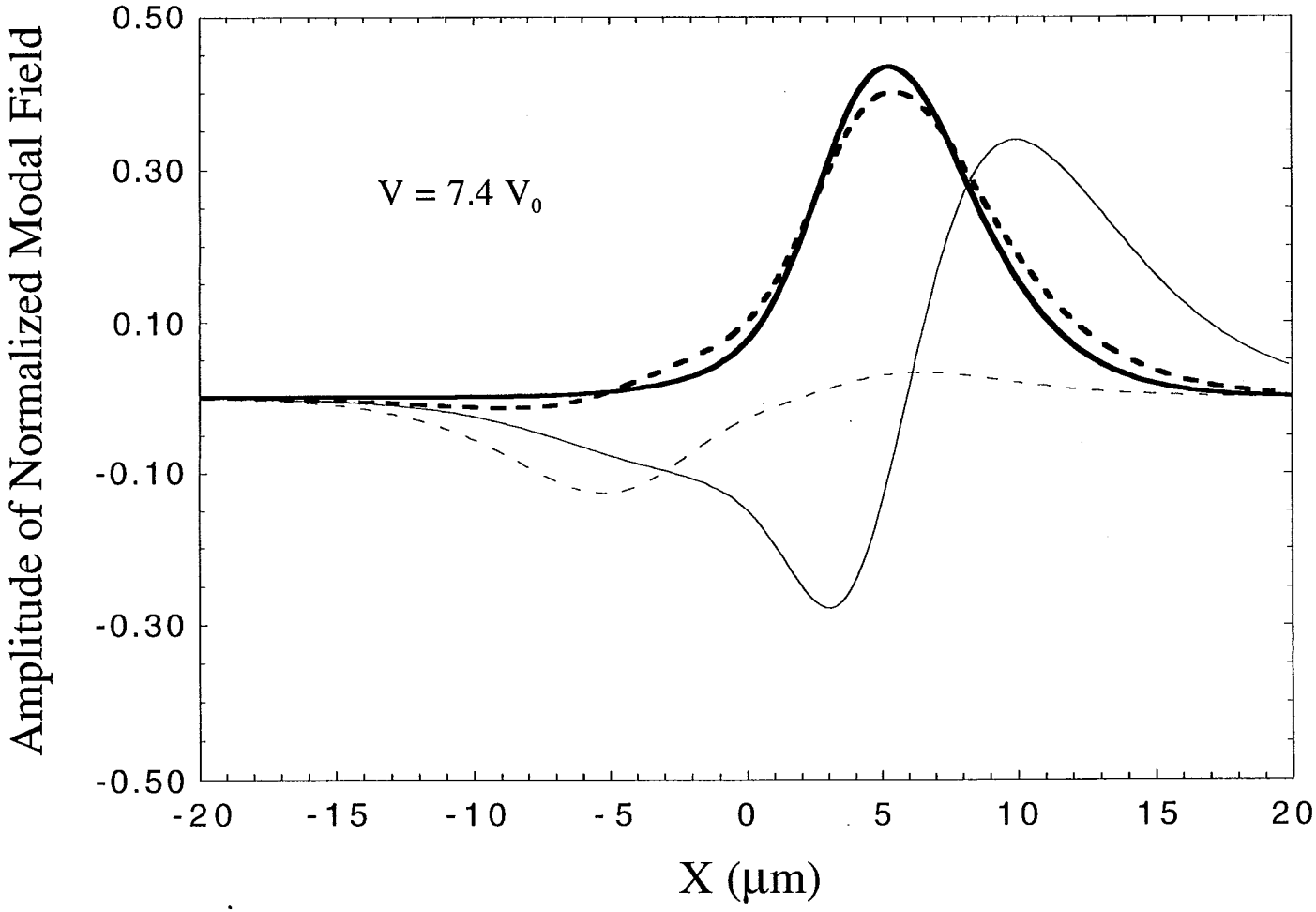
Amplitude of Normalized Modal Field
0.50
0.30
0.10
-0.10
-0.30
-0.50
V = 7.4 V0
-20
-15
-10
-5
0
5
10
15
20
X (μm)

Fig 5 (e)

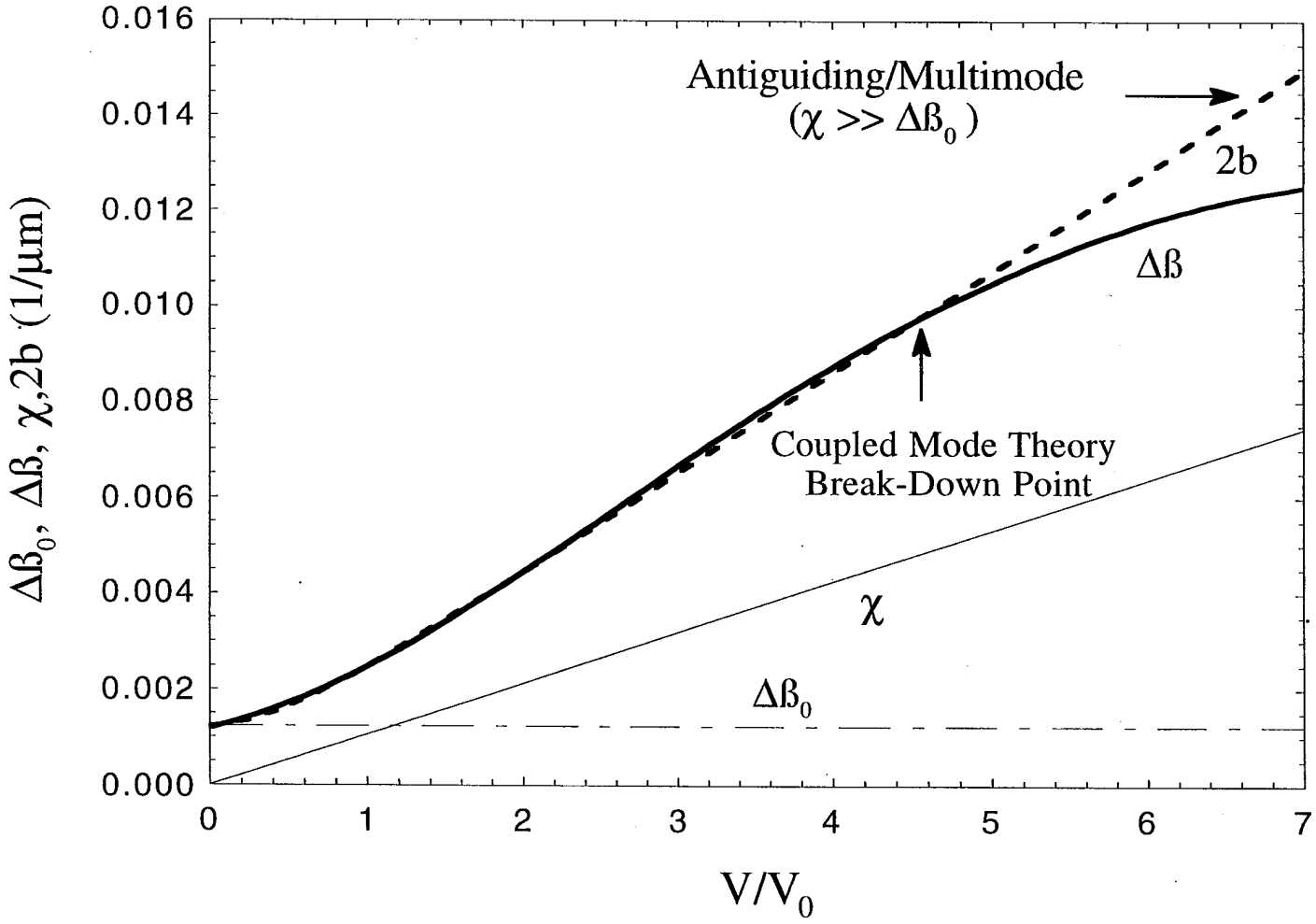
0.016
0.014
0.012
0.010
0.008
0.006
0.004
0.002
0.000
0
1
2
3
4
5
6
7
Δß0, Δß, χ,2b (1/μm)
V/V0
Antiguiding/Multimode
(χ >> Δß0)
2b
Δß
Coupled Mode Theory
Break-Down Point
χ
Δß0

Fig. 6

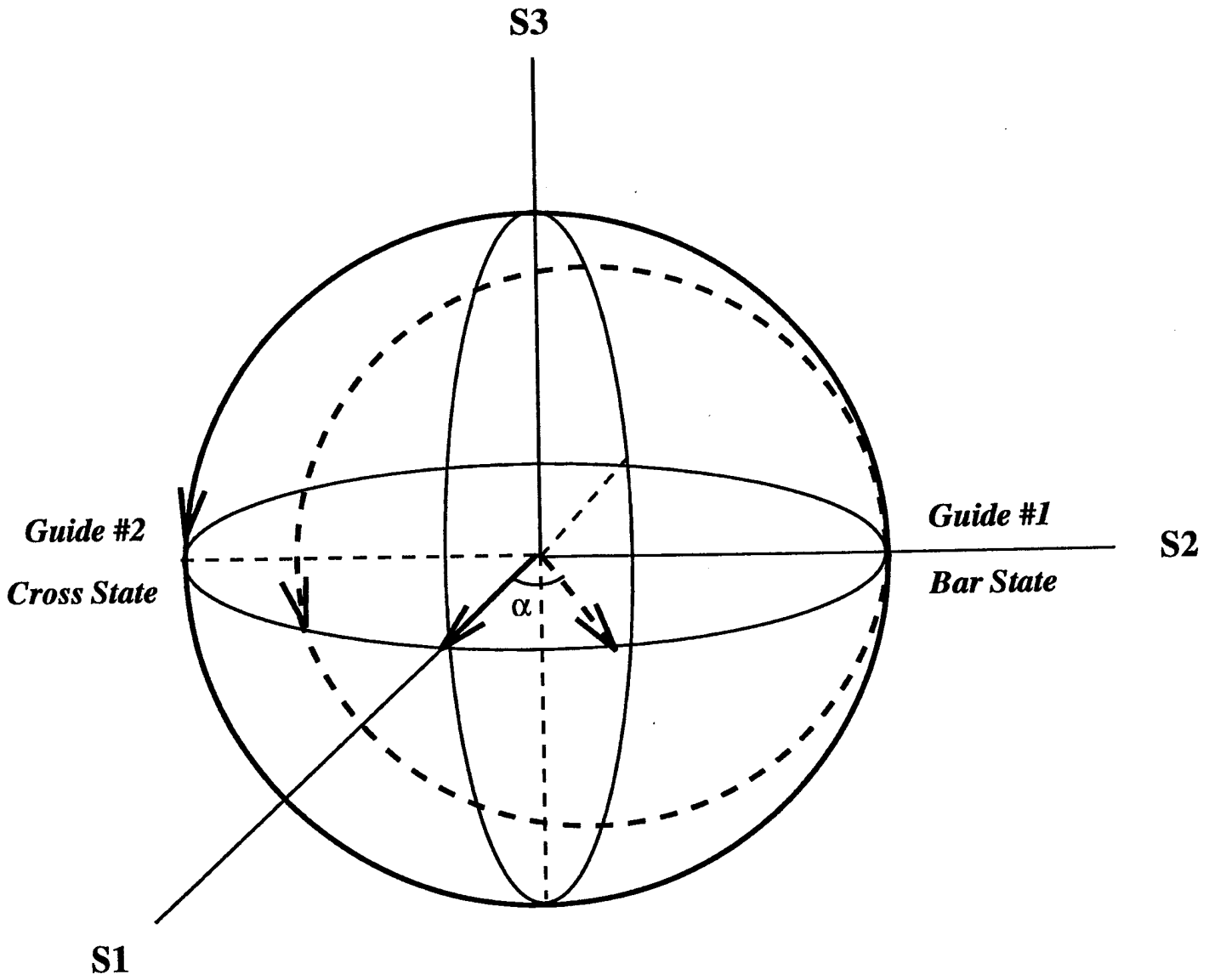

Fig. 7

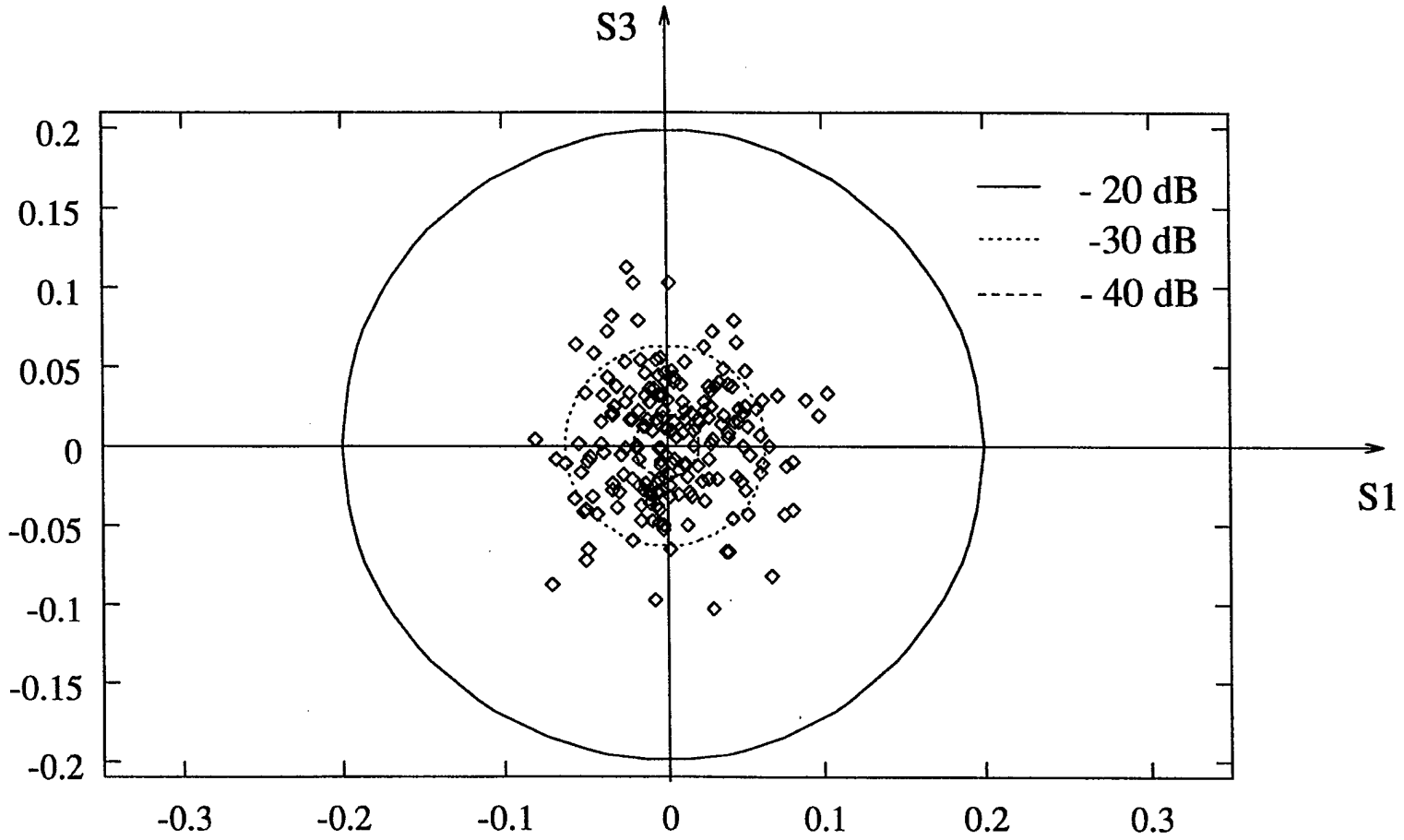
S3
S1
0.2
0.15
0.1
0.05
0
-0.05
-0.1
-0.15
-0.2
-0.3
-0.2
-0.1
0
0.1
0.2
0.3
- 20 dB
-30 dB
- 40 dB

Fig. 8 (a)

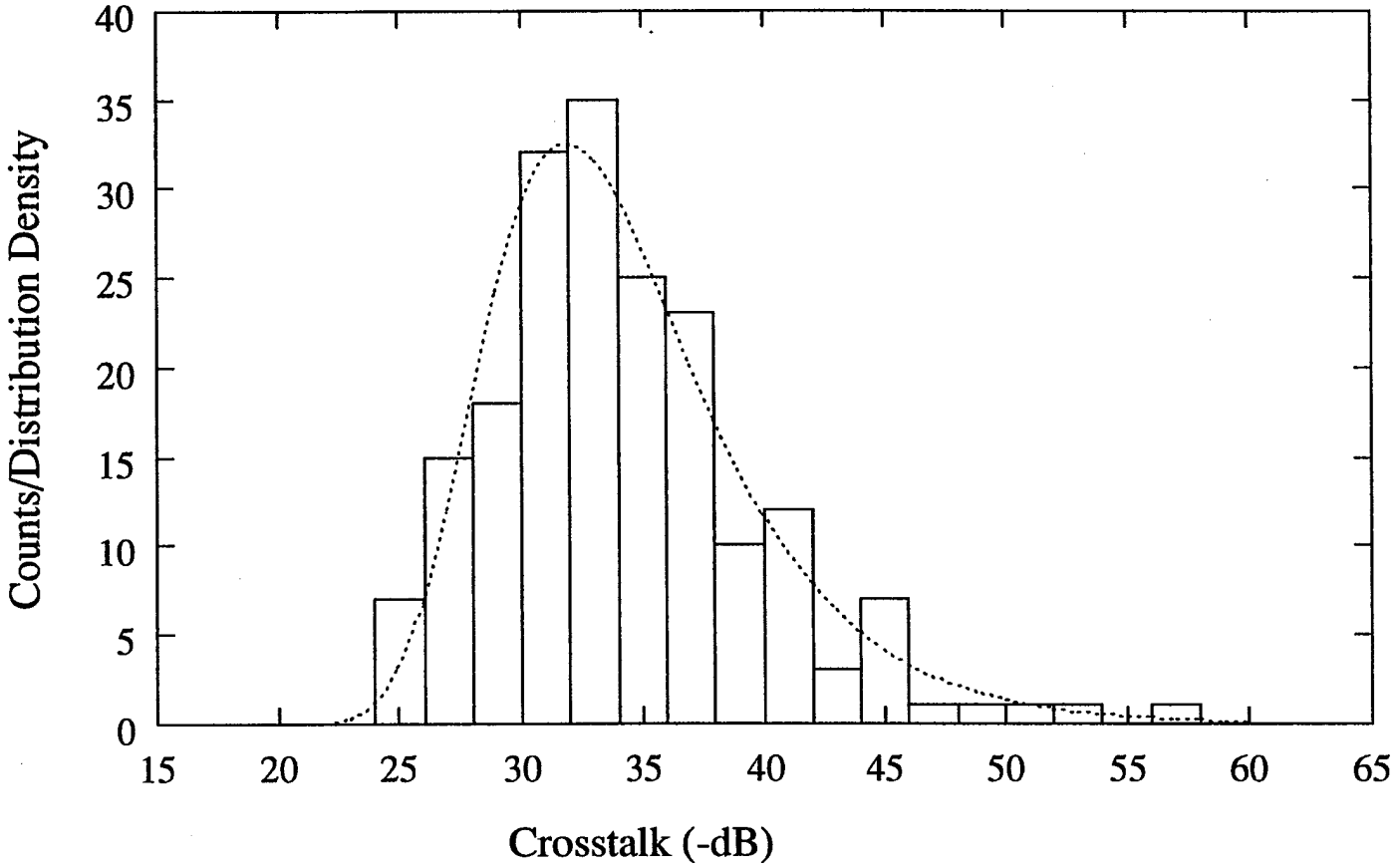
Counts/Distribution Density
0
5
10
15
20
25
30
35
40
15
20
25
30
35
40
45
50
55
60
65
Crosstalk (-dB)

Fig. 8(b)

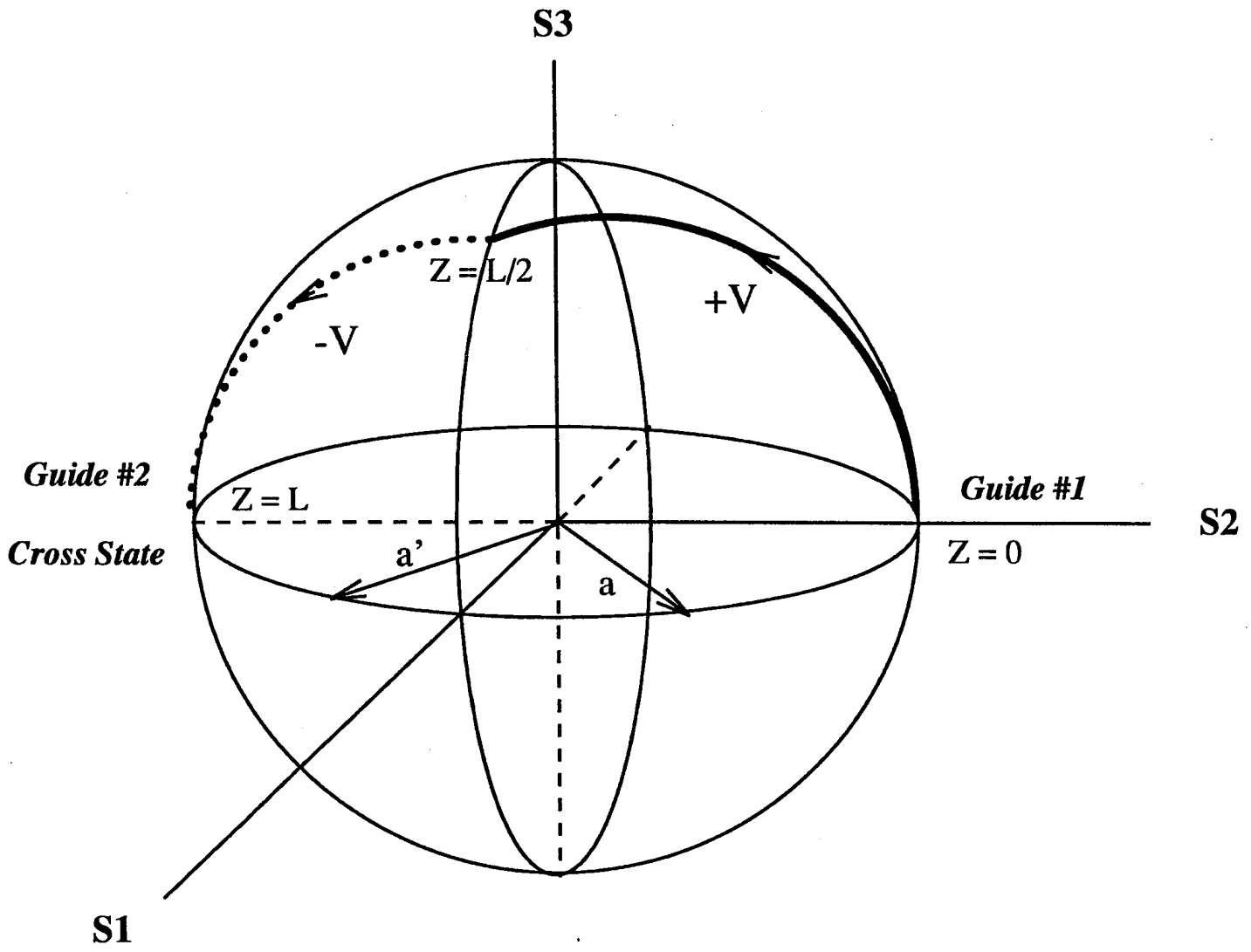

Fig. 9 (a)

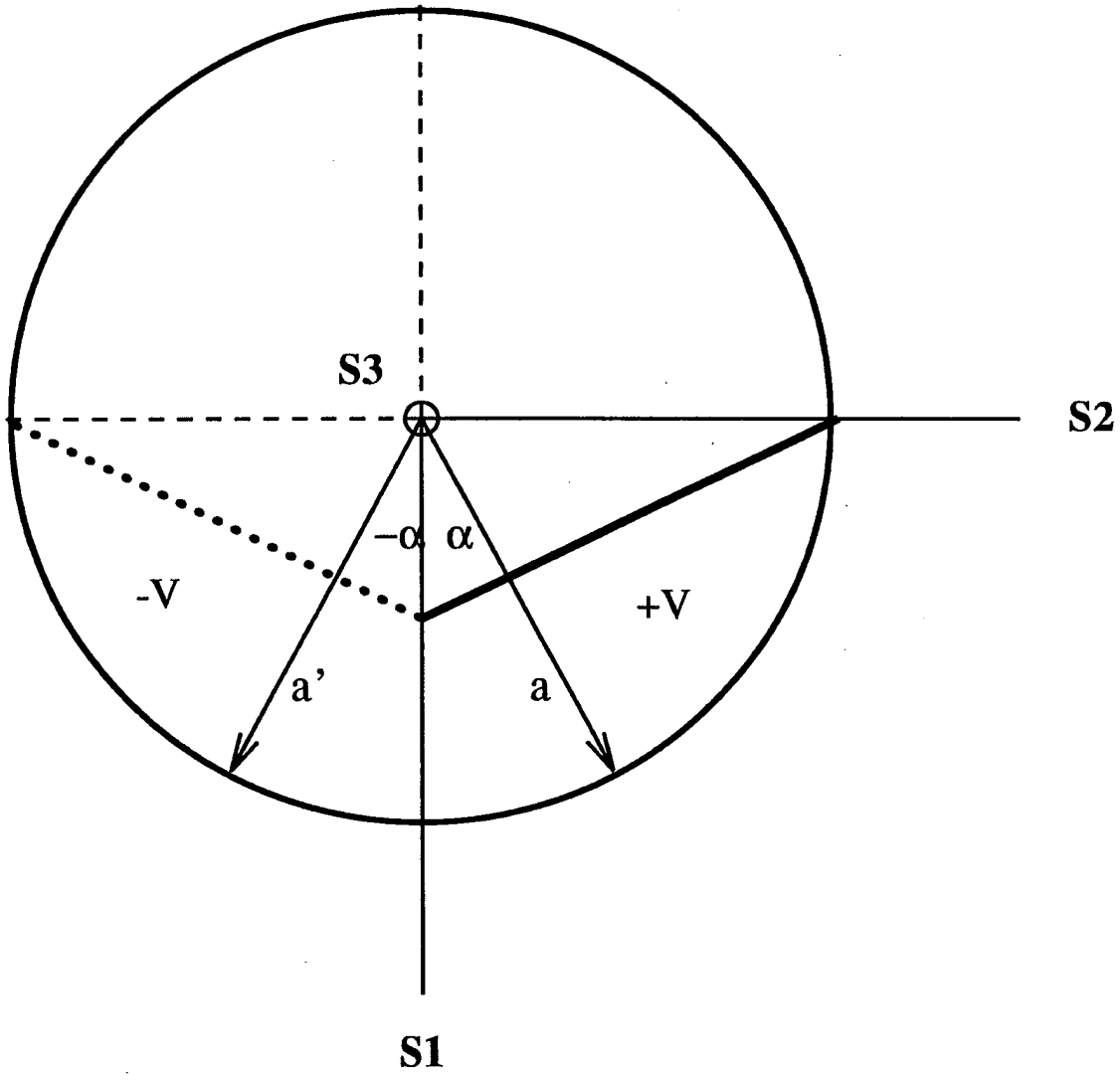

Fig. 9 (b)

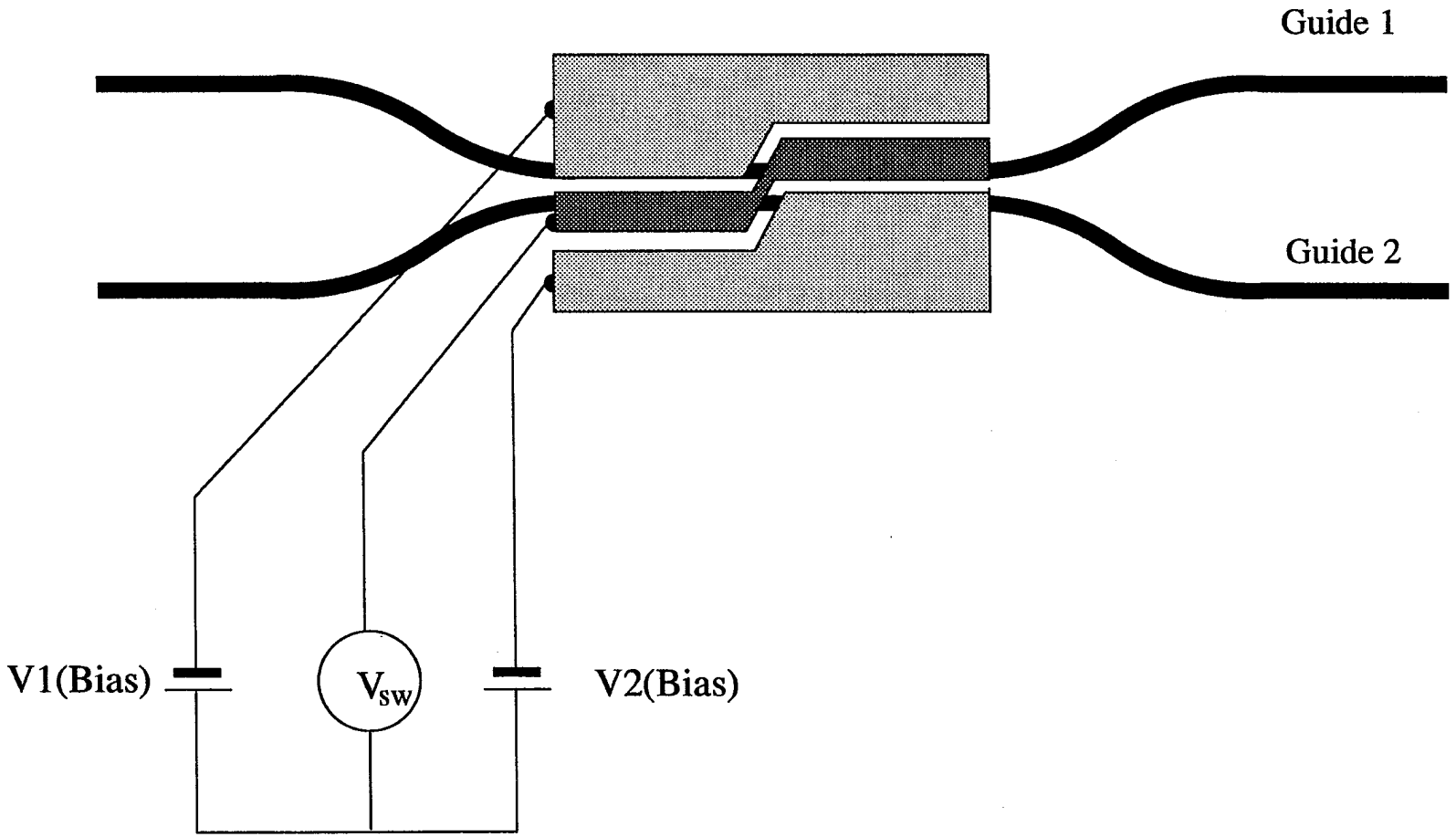

Fig. 10 (a)

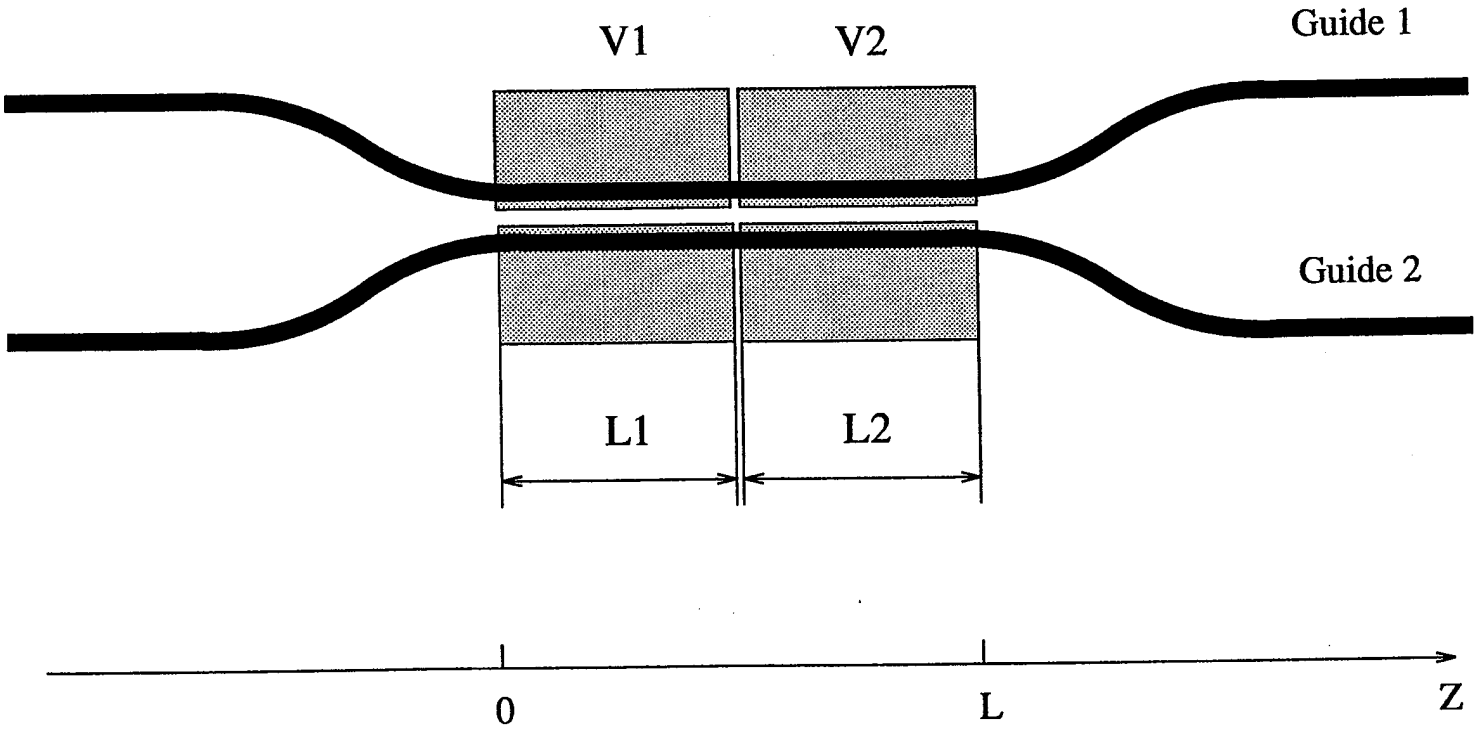

Fig. 10 (b)

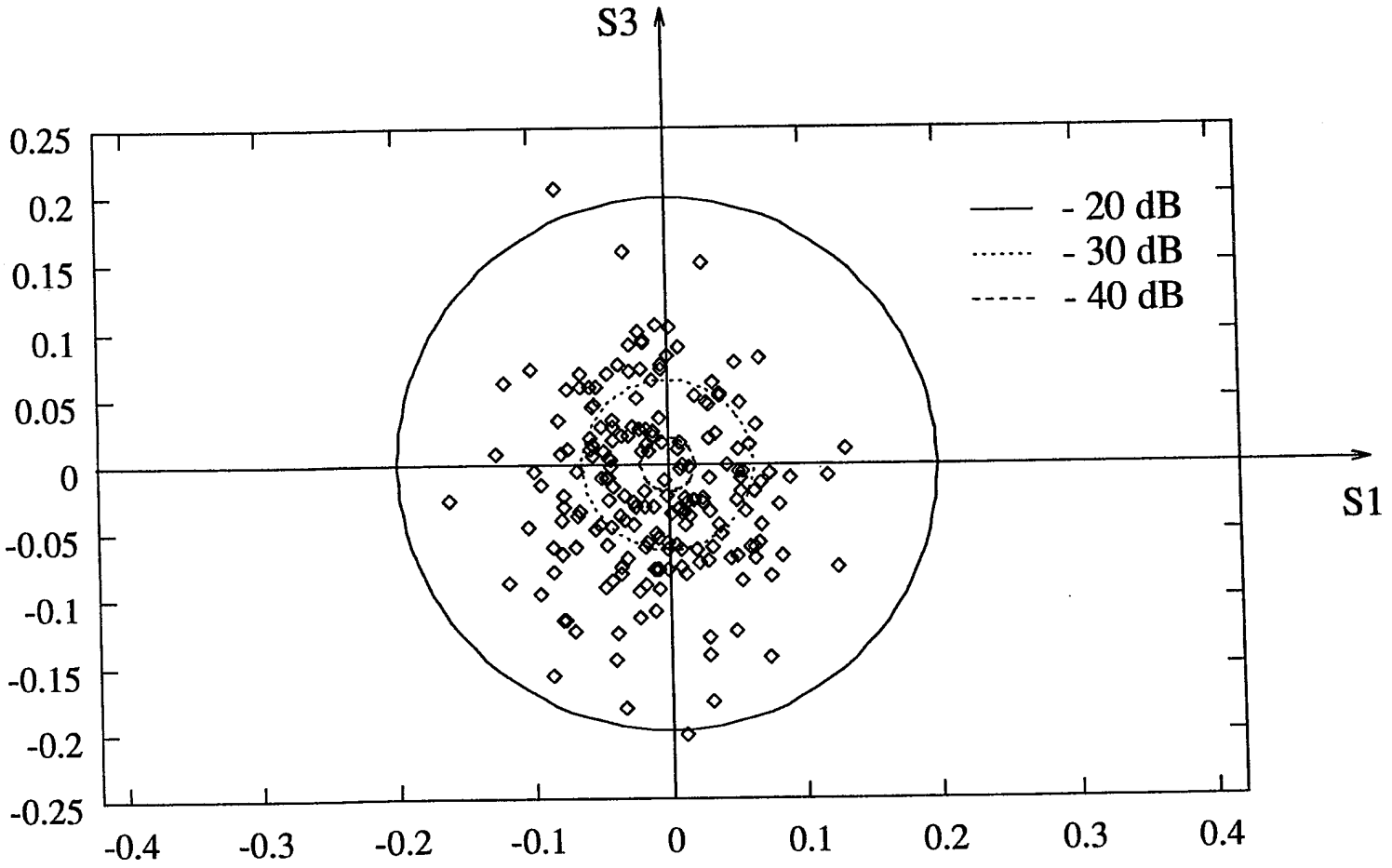
S3
S1
0.25
0.2
0.15
0.1
0.05
0
-0.05
-0.1
-0.15
-0.2
-0.25
-0.4
-0.3
-0.2
-0.1
0
0.1
0.2
0.3
0.4
- 20 dB
- 30 dB
- 40 dB

Fig. 11 (a)

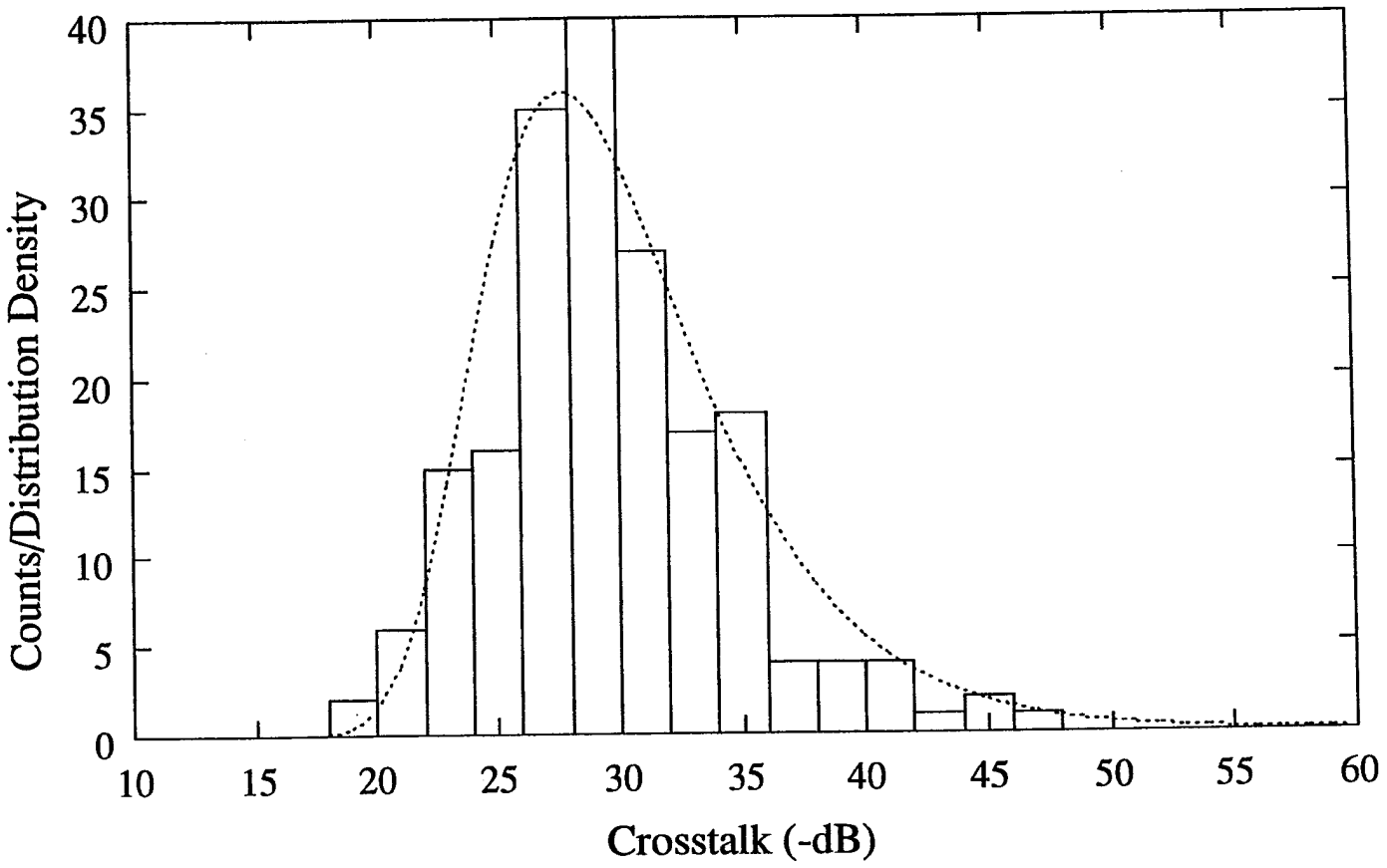
Counts/Distribution Density
0
5
10
15
20
25
30
35
40
10
15
20
25
30
35
40
45
50
55
60
Crosstalk (-dB)

Fig. 11 (b)

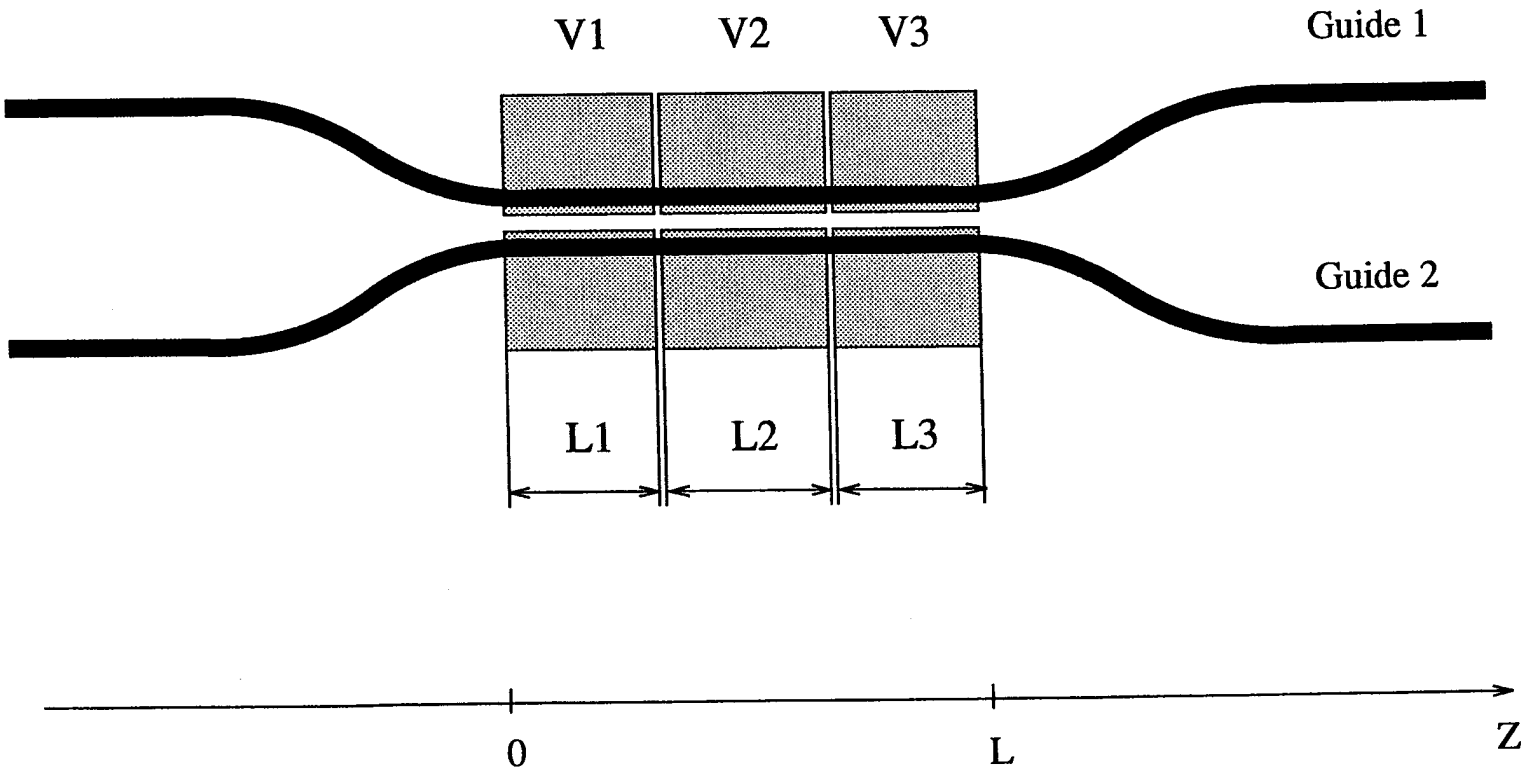

Fig. 12